

Video Influencers: Unboxing the Mystique

Prashant Rajaram*
Puneet Manchanda

June 2020

This Version: January 28, 2023

* Rajaram (prajaram@ivey.ca) is Assistant Professor of Marketing at the Ivey Business School, Western University, and Manchanda (pmanchan@umich.edu) is Isadore and Leon Winkelman Professor and Professor of Marketing, at the Stephen M. Ross School of Business, University of Michigan. The authors would like to thank David Jurgens, Mengxia Zhang, Eric Schwartz, Zhenling Jiang, Jun Li, Yiqi Li, Yu Song, the Marketing faculty and doctoral students at the Ross School of Business, seminar participants at Ivey Business School, University of Wisconsin-Madison, Singapore Management University, Bocconi University, National University of Singapore, University of Manitoba, Bass FORMS Conference 2021, AIM Conference 2021, ISMS Marketing Science Conference 2021, Joint Statistical Meeting 2021, KDD 2021, ISMS Doctoral Consortium 2022 and MSI Webinar 2022 for their valuable comments and feedback.

Abstract

Influencer marketing has become a very popular tool to reach customers. Despite the rapid growth in influencer videos, there has been little research on the effectiveness of their constituent elements in explaining video engagement. We study YouTube influencers and analyze their unstructured video data across text, audio and images using a novel “interpretable deep learning” framework that accomplishes both goals of prediction and interpretation. Our prediction-based approach analyzes unstructured data and finds that “what is said” in words (text) is more influential than “how it is said” in imagery (images) followed by acoustics (audio). Our interpretation-based approach is implemented after completion of model prediction by analyzing the same source of unstructured data to measure importance attributed to the video elements. We eliminate several spurious and confounded relationships, and identify a smaller subset of theory-based relationships. We uncover novel findings that establish distinct effects for measures of shallow and deep engagement which are based on the dual-system framework of human thinking. Our approach is validated using simulated data, and we discuss the learnings from our findings for influencers and brands.

Keywords: *Influencer Marketing, Video Advertising, Social Media, Interpretable Deep Learning, Transfer Learning*

1. Introduction

Influencers have the capacity to shape the opinion of others in their network. They were traditionally celebrities (e.g., movie stars and athletes) who leveraged their expertise, fame and following in their activity domain to other domains. However, 95% of the influencers today, or “social media stars,” are individuals who have cultivated an audience over time by making professional content that demonstrates authority and credibility (O'Connor, 2017). The growth in their audience(s) has been in part attributed to the fact that influencer videos are seen as “authentic” based on a perception of high source credibility. The increasing popularity of social media stars has resulted in an exponential growth of the influencer marketing industry which is expected to reach a global valuation of \$22.2B in 2025 from \$9.7B in 2020 (Statista, 2023). There are now more than 18,000 influencer marketing agencies in the world that allow brands to partner with influencers to promote their products (Influencer Marketing Hub, 2022). These influencers primarily reach their audience(s) via custom videos that are available on a variety of social media platforms (e.g., YouTube, Instagram, and TikTok) (Brooks, 2020). Despite the rapid emergence and growth of influencer videos, there is limited research on the effectiveness of their constituent elements. Specifically, little is known about the impact of different video elements across text, audio and images in building video engagement. In this paper, we investigate this by developing a novel “interpretable deep learning” framework that comprises two approaches – prediction and interpretation.

First, we use the prediction-based approach to investigate the relative influence of structured data and unstructured data – text, audio and images – in videos in explaining engagement with the video. Second, we adapt the theoretical framework of attention capture and transfer from the print advertising literature (Pieters & Wedel, 2004) to our setting and interpret the association between theory-based stimuli (in text, audio and images) and engagement. There are three main challenges in carrying out these tasks. First, most data in influencer videos are unstructured and span different modalities – text, audio and images. This necessitates the use of state-of-the-art machine learning methods customized for each type of unstructured data. The second challenge arises from the fact that past approaches in marketing using such methods have documented a tradeoff between predictive ability and interpretability (Dzyabura et al., 2022; Liu et al., 2020; Liu et al., 2019). Specifically, deep learning models that use unstructured data as input predict marketing outcomes well out-of-sample but suffer from poor interpretability. On the other hand, deep learning models that use ex-ante handcrafted features as input obtain high interpretability of the captured relationships but suffer from poor predictive ability. We develop an “interpretable deep learning” framework that avoids making this tradeoff. Specifically, we use unstructured data across multiple modalities as input to our deep learning models, make predictions and then ex-post peek inside the machine learning “black box” to interpret the captured relationships. Finally, the analysis of unstructured data is computationally very demanding. We overcome this challenge using “transfer

learning” methods that also prevent overfitting and aid in interpretation of the captured relationships. We apply our framework to publicly available influencer videos on YouTube, the platform where influencers charge the most for a post (Klear, 2019; McClure, 2020).

We use a random sample of 1620 videos scraped from 33 YouTube influencers (across 11 product categories) who obtain revenue from brand endorsements. We analyze these videos using transfer learned models with novel customized architectures. Using a unique model for each source of unstructured data (text, audio or images), we capture their relationship with measures of engagement. We then combine information from each model of unstructured data with structured features to study the relative importance of each source of data. Our engagement measures are divided into measures of shallow engagement (System I) and deep engagement (System II) which are motivated by Kahneman’s work on frames of intuitive and deliberate thinking respectively (Kahneman, 2003). The use of these measures is also supplemented by industry practice and past research in advertising and social media (Goh et al., 2013; Influencer Marketing Hub, 2022; Mitchell, 1986) (see Section 4.2 for details).

We develop a novel ex-post interpretation approach that peeks inside our machine learning models after the end of prediction to interpret the relationships that have been captured between theory-based stimuli and our measures of engagement. Our theory-based stimuli comprise text elements (e.g., brand and emotional words), audio elements (e.g., speech and music) and image elements (e.g., human images and packaged goods). Our interpretation approach is based on the attention capture and transfer framework of Pieters and Wedel (2004), and we implement it as follows. First, we find correlations between theory-based stimuli and the importance measures attributed by our model to these stimuli. Doing so allows us to identify whether elements in text, audio or images play an important role in predicting engagement. However, some of these correlations may be spurious due to peculiarities in the design of deep learning models (Vashishth et al., 2019). In the second step, we validate whether there exist correlations between theory-based stimuli and the engagement measures predicted by our model. However, some of these correlations may be confounded by unobserved variables. Hence, we shortlist relationships that are correlated in both steps, and end up eliminating many spurious and confounded relationships. Thus, we identify a subset of relationships, which are more likely to have external validity, for further formal causal testing. Our identified relationships and interpretation approach are also validated by theoretical expectations and multiple robustness checks including simulations.

Our prediction results demonstrate that unstructured data in text (captions/transcript) (across the beginning, middle and end of a video) captures more variation in all the engagement measures than unstructured data in images (video frames) and audio. This shows that “what is said” in words is more influential than “how it is said” in imagery and acoustics. Furthermore, when conveying information, we find that imagery is more important than acoustics in explaining engagement. We also find that on

average, stimuli in the beginning of videos explain more variation in engagement than stimuli in the middle or end of videos. This demonstrates that stimuli in the beginning of the viewing experience are typically most salient, which is consistent with findings in prior research for ad videos (Tellis et al., 2019). Our findings empower influencers by providing them general directions along which design efforts can be prioritized so that improvements in engagement are most likely. Finally, we also demonstrate that our interpretable framework does not compromise the predictive ability of our model.

Our results from ex-post interpretation uncover some interesting findings. First, we find that mentioning brand names, especially in the electronics and digital categories, in captions/transcript in the beginning 30 seconds is more often associated with an increase in importance directed to the brand name and an increase in the sentiment of *automatic* reactions (System I) but a decrease in the sentiment of *deliberate* reactions (System II). This suggests presence of heterogeneity in viewer response based on their frame of thinking. We also find that an increase in size of human images (and packaged goods) in the video frames displayed in the beginning 30 seconds is associated with an increase (and decrease) in the sentiment of *automatic* reactions (System I). This can be explained by the desire to socialize, engage and communicate with other humans. Overall, our findings from ex-post interpretation are broadly consistent with findings on related domains in previous literature, but are also novel in their ability to distinguish between effects on shallow (System I) and deep (System II) engagement.

Our results are relevant for multiple audiences. For academics, who may be interested in testing causal effects, our novel ex-post interpretation approach is able to identify a smaller subset of theory-based relationships for formal causal testing. For practitioners, we provide a general approach to the analysis of videos used in marketing that does not rely on time-consuming primary data collection and can be undertaken with secondary data. For brands, influencers and agencies, our results provide a theory-based understanding of the association between video features and relevant measures of deep and shallow engagement. Brands and agencies can also evaluate different influencer videos using our video scoring system and assess potential partnership opportunities.

Overall, this paper makes five main contributions. First, to the best of our knowledge, it is the first paper that rigorously documents the relative contribution of individual sources of unstructured data (across text, audio and images) in influencer videos while predicting engagement with the videos. Second, and most importantly, it develops a novel “interpretable deep learning” framework that uses unstructured data to make good out-of-sample predictions and then peeks inside the same framework to interpret the captured relationships. This allows usage of the same source of unstructured data for both *prediction* of engagement and also *interpretation* of the association between theory-based stimuli and engagement. Third, it adapts the attention transfer and capture framework from the advertising literature for use in the influencer video setting to interpret relationships using secondary data. Our novel interpretation approach

eliminates spurious relationships due to model artifacts and confounding factors unassociated with importance directed to the stimuli. This results in a smaller subset of relationships which can be validated by theory and which can also be further validated in future work by formal causal testing. Fourth, it presents novel substantive findings that uncover distinct effects for measures of deep and shallow engagement which relate with theory on human thinking. Finally, it provides a comprehensive approach for marketers to assess and evaluate the quality of long-form videos (across multiple domains such as entertainment, education and politics) using secondary data.

The remainder of the paper is organized as follows. Section 2 discusses the related literature while Section 3 details our theoretical frameworks and theory-based stimuli. Section 4 describes the data used for analysis, Section 5 details the models for analyzing unstructured and structured data, and Section 6 discusses our ex-post interpretation approach. The results and robustness checks are described in Section 7 while the implications of our approach/findings for influencers and marketers are described in Section 8. Section 9 concludes with a discussion of the limitations and directions for future research.

2. Related Literature

In this section, we review the literature on influencer marketing and unstructured data analysis (using deep learning) and describe how our work builds on it.

2.1 Influencer Marketing

The growing literature on influencer marketing has analyzed influencer marketing effectiveness across text, audio and video data. Influencer marketing literature that analyzes textual data has found that high influencer expertise on sponsored blog posts is more effective in increasing comments below the blog if the advertising intent is to raise awareness versus increasing trial (Hughes et al., 2019). Zhao et al. (2019) study the audio transcript of live streamers on the gaming platform Twitch, and find that lower values of conscientiousness, openness and extraversion but higher values of neuroticism are associated with higher views. Leung et al. (2022) study influencer text posts on Weibo and find that an increase in brand mentions are associated with an increase in the post's informativeness and result in an increase in reposts.

Use of audio and video data in influencer marketing research has gained increasing prominence in recent years. Hwang et al. (2021) find that influencers on Instagram use a softer voice in sponsored videos which can help increase the sentiment in comments below the post. Cheng and Zhang (2022) find that sponsored videos on YouTube by beauty and style influencers lead to a loss in subscribers as compared to organic videos created by them, and similarly Chen et al. (2022) find that early brand disclosure in influencer videos on Bilibili is associated with a reduction in the sum of likes, comments and shares for the video. On TikTok, Yang et al. (2021) find that a product that is advertised in the most engaging parts

of a video leads to higher sales, and Tian et al. (2022) find that an increase in followers leads to an increase in impressions. Lanz et al. (2019) study network effects on a leading music platform, and find that unknown music creators can increase their follower base by seeding other creators with less followers than creators who are influencers (with more followers). Huang and Morozov (2022) study influencers on Twitch and find that their sponsored streams result in an increase in game sales. Using a theory model, Pei and Mayzlin (2022) model the extent of the affiliation decision between the brand and the influencer, and show that when a consumer's prior belief about product-influencer fit is high, the brand affiliates completely with the influencer to maximize awareness and prevent a negative review.

In our paper, we add to the literature on influencer marketing by focusing on the role of unstructured data—text, audio and images—in YouTube influencer videos in promoting video engagement. We uncover the relative importance of these sources of unstructured data, and then interpret the relationship between theory-based stimuli (within text, audio or images) and video engagement.

2.2 Unstructured Data Analysis in Marketing via Deep Learning

The use of deep learning methods to analyze unstructured data in the marketing literature has gained increasing prominence in recent years due to its ability to capture complex non-linear relationships that help make better predictions on outcomes of interest to marketers. Marketing research on textual data has used combinations of Convolutional Neural Nets (CNNs) and Long Short-Term Memory Cells (LSTMs) to study various outcomes including sales conversion at an online retailer (Liu et al., 2019), whether Amazon reviews are informative (Timoshenko & Hauser, 2019), sentiment in restaurant reviews (Chakraborty et al., 2022) and restaurant survival (Zhang & Luo, 2022). Research on image data has also used CNNs but within more complex architectures such as VGG-16 to classify and label images (Hartmann et al., 2021; Zhang et al., 2021), Caffe framework to predict brand personality (Liu et al., 2020) and ResNet152 to predict product return rates (Dzyabura et al., 2022).

Marketing literature has also applied deep learning on video data. Engineered features have been extracted from images, audio or text of video data to study their relationship with various outcomes, such as product preference while shopping (Lu et al., 2016), project success on Kickstarter (Li et al., 2019), consumer sentiment on Instagram (Hwang et al., 2021), video completion of educational courseware (Zhou et al., 2021) and number of subscribers on YouTube (Cheng & Zhang, 2022). Transfer learning has also been applied on video data to find the most engaging parts of the video that increase product sales on TikTok (Yang et al., 2021). There has also been research that embeds information from different data modalities using deep learning methods to create unified multi-view representations. Combinations of structured data and text have been used to predict business outcomes (Lee et al., 2022), brand logo images and textual descriptions have been combined to suggest logo features for a new brand (Dew et al., 2022),

car designs have been combined with ratings data to suggest new designs (Burnap et al., 2021), and unstructured data from TikTok videos has been embedded in lower dimensional space to use as a control variable (Tian et al., 2022). The marketing literature has also documented that deep-learning models that self-generate features have better predictive ability than those that use ex-ante hand-crafted features (Dzyabura et al., 2022; Liu et al., 2020; Liu et al., 2019). While hand-crafted features suffer from poor predictive ability, they allow interpretability of their effect on the outcome variable. We avoid this tradeoff by developing an “interpretable deep learning” framework that accomplishes both goals of prediction and interpretation, and thus substantially extend the work in prior literature.

3. Theoretical Frameworks

We explain our theoretical frameworks in 3.1 and 3.2, and describe our theory-based stimuli in 3.3.

3.1 Interpretable Deep Learning Framework

Deep learning models are especially suited to analyze unstructured data (text, audio and images) as they can efficiently capture complex non-linear relationships and perform well in prediction tasks (Dzyabura & Yoganarasimhan, 2018). However, they are perceived as a “black box” that offer little interpretability of the captured relationships. This is because the features that are self-generated by deep learning models from unstructured data are difficult to interpret. On the other hand, ex-ante engineered features from unstructured data are structured features (e.g., number of words in text, image brightness, loudness in voice, etc.) which when passed as input to deep learning models are known to have poor predictive ability as they neither identify a comprehensive set of important features nor capture all the underlying latent constructs. However, they offer greater interpretability of the captured relationships because we can observe a change in outcome for a unit change in a structured feature.

This tradeoff between predictive ability and interpretability has been well documented in prior research (Dzyabura et al., 2022; Liu et al., 2020; Liu et al., 2019). We overcome this tradeoff using our “interpretable deep learning” framework shown in Figure 1. We use unstructured video data as input to a set of deep learning models that predict engagement with a video. Training deep learning models from scratch can be computationally very demanding and can lead to overfitting unless one has superior computational resources and millions of data points respectively (typically only available to big companies). Hence, to circumvent these issues, we use a transfer learning approach. First, we use a base (deep-learned) model (for each source of unstructured data - text, audio or images) that has been pre-trained in previous machine learning literature on a separate task with millions of observations at a very high computational cost. On top of the base models, we implement novel customizations and design architectures (Section 5) that help with prediction (and ex-post interpretation). We then finetune the models to capture the relationship between different sources of unstructured video data (text, audio and

images) in our sample and our measures of engagement. As we use unstructured video data as input, we are able to achieve predictive ability (results in Section 7.1).

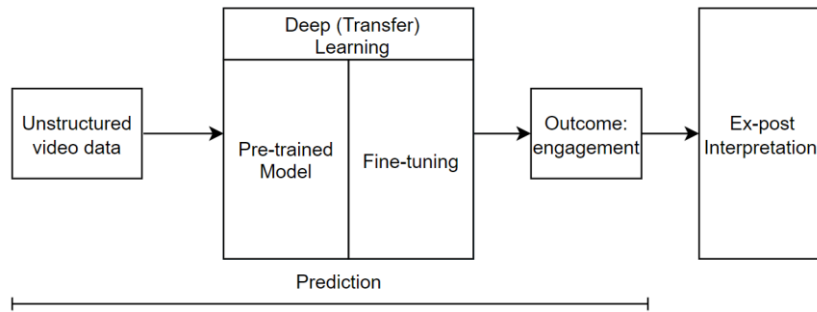


Figure 1: Interpretable Deep Learning Framework

Now, transfer learning also aids in interpretation. This is because the transfer learned models have pre-learned basic features for text, audio and images (e.g., contextual usage of words, differences in sound classes and distinctive characteristics of images) by virtue of being trained on millions of observations (Weiss et al., 2016). Hence, during finetuning, our transfer learned models can easily capture word context, sound classes and image characteristics in our sample of influencer videos. After completing prediction, we implement ex-post interpretation by “peeking” inside the trained model to uncover the captured relationships. We accomplish this by engineering features (stimuli) ex-post from the unstructured data which were supplied as input to the deep learning models, and then study the *attention* (importance) attributed by the model to these stimuli while originally predicting engagement. Hence, our framework also allows for interpretation of the captured relationships (results in Section 7.2). We explain the theory behind interpretation in 3.2.

3.2 Ex-Post Interpretation Framework

To the best of our knowledge, there is no extant theoretical framework that links the impact of influencer videos to their constituent elements. In this paper, we propose such a framework that is an adaption of the theoretical framework describing attention capture and transfer in print advertising in Pieters and Wedel (2004). This framework describes the effect of bottom-up (automatic) factors and top-down (volitional) factors that can affect attention to ad elements. In primarily “entertainment commerce” platforms, such as YouTube and TikTok, bottom-up attention (or saliency-based attention) is more likely to be exhibited by viewers compared to top-down attention which is more volitional and more commonly occurs in search driven product markets (Yang et al., 2021). Viewers primarily come to such platforms for entertainment (Google, 2016), and salient elements in videos are more likely to grab viewer’s bottom-up attention. These salient elements could be in either text, audio or images. The part of the framework of Pieters and Wedel (2004) that is directly relevant for our influencer video setting is shown in Figure 2.

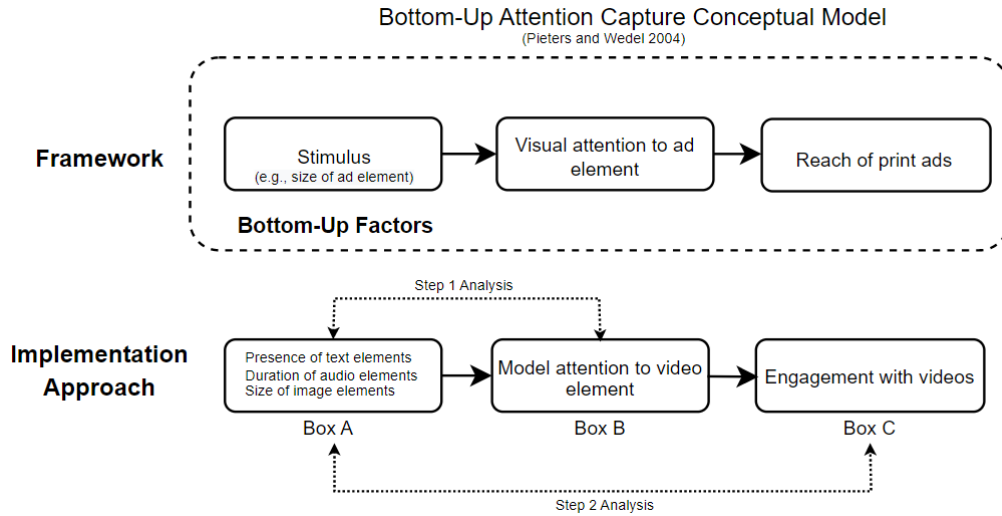


Figure 2: Ex-Post Interpretation Framework

The figure illustrates the bottom-up attention capture conceptual model, where a stimulus such as the size of an ad element directly affects attention to the ad. This in turn can have a direct effect on reach of print ads. For example, Pieters and Wedel (2004) find that surface size of the text area in print ads is superior to the surface size of the image (pictorial) area in drawing attention to the whole ad. We describe our approach to implement their framework in the bottom half of Figure 2. The stimuli in our setting comprise the presence of text elements, duration of audio elements or size of image elements in influencer videos (Box A) (detailed in Section 3.3). We capture *model attention* (not viewer visual attention) to these elements (Box B) using independent deep learning models for each source of unstructured data (text, audio or images). These models are more attentive to those stimuli (ex-post features) in videos that explain better variation in engagement (Box C).¹

Our analysis is carried out in two steps. In Step 1, we find correlations between the stimuli (Box A) and the *importance* (attention) attributed to the stimuli (Box B) while training our deep learning models. The idea is that if the stimuli are important in predicting engagement, then the model must assign more *importance* to these stimuli. By studying these correlations, we are able to identify whether stimuli in text, audio or images play an important role in predicting engagement. However, some of these correlations may potentially be spurious due to peculiarities (artifacts) in the design of deep learning models (Vashishth et al., 2019; Wiegrefe & Pinter, 2019). In Step 2, we find correlations between the stimuli (Box A) and the predicted engagement measures that have been returned by our deep learning

¹ The framework in Pieters and Wedel (2004) uses eye-tracking studies to measure visual attention. We complement this stream of work by analyzing secondary data, and introduce the concept of *model attention* from the machine learning literature to the marketing literature. Our approach is able to analyze a lot more seconds of data than what is used in traditional eye tracking studies. Moreover, our approach can be applied on public videos that potentially engage millions of viewers, as opposed to the small number of viewers in conventional lab or field studies. It is also important to note that model attention is not independent of eye tracking attention, and extant research in machine learning has found that they have a statistically significant correlation (Selvaraju et al., 2017).

models (Box C). The idea is that if the stimuli are truly important in predicting engagement, then they must be correlated with the value of engagement predicted by the deep learning models. However, some of these correlations may be confounded by unobserved variables. Hence, we find relationships that fall at the intersection of Step 1 and Step 2. This is visually illustrated using a Venn diagram in Figure 3.

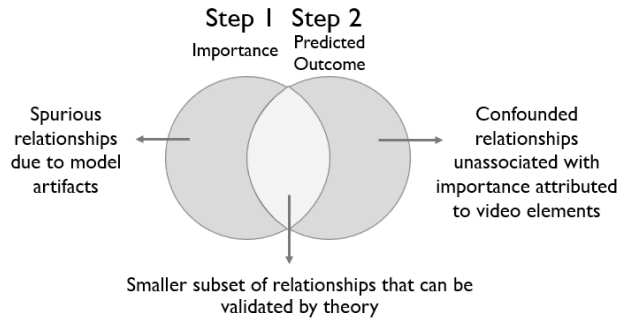


Figure 3: Implementation of Ex-Post Interpretation

In other words, we identify the stimuli (Box A) that result in both an increase in attention (Box B) and a change in the predicted outcome (Box C). Note that in Step 2, we use the predicted outcome and not the observed outcome to study correlations with theory-based stimuli. This is because the predicted outcome has been influenced by the (estimated) importance measures, and hence, using predicted outcome as the dependent variable in Step 2 will be directly comparable with the analysis in Step 1 that uses (estimated) importance measures as the dependent variable. By using a two-step process, we are able to eliminate several spurious relationships (from Step 1) and confounded associations (from Step 2), and identify a subset of relationships that are more likely to have external validity and can be validated by theory. We detail this theory in Section 3.3, and detail the two-step process in Section 6.

3.3 Theory-based Stimuli

We would like to choose stimuli or features that can be locally identified (as salient regions) within text, audio or images so that they can be used within the theoretical framework of Figure 2. For example, a person in an image can be locally identified but the brightness of an image refers to the entire image and is not a local aspect of an image (Dzyabura et al., 2022; Li et al., 2019; Zhang et al., 2021). We narrow our focus to those local features which can drive a change in the sentiment of engagement as guided by theory (in past literature) and which are also likely to be of interest to marketers and brand partners. We elaborate on these features below and summarize the corresponding theory-based expectations in Table 1.

3.3.1 Presence of text elements

Viewers like viewing ads which have high entertainment value and low informational value (Wilbur, 2016; Woltman Elpers et al., 2003). Similarly, viewers view influencer videos for their entertainment value (Landsberg, 2021). As discussed earlier, stimuli in entertaining videos can activate bottom-up

Unstructured data	Stimuli in Unstructured data	Theory	Literature	Expected change in sentiment of engagement
Text: Captions/ Transcript	Presence of brand names	Brand mentions may lower entertainment value and decrease persuasiveness of message. Brand mentions may increase informational value and increase viewers' trust in the brand.	Tellis et al. 2019; Teixeira et al. 2010 Leung et al. 2002; Lou and Yan 2019	Unknown
	Presence of emotional words	Emotional words are tied to a brand's personality, evoke high arousal and increase persuasiveness of the message. Emotional words are associated with disingenuous persuasion or insincerity and signal fakeness.	Lee et al. 2018; Berger & Milkman 2012 Bakir & McStay 2018; Guo et al. 2019	Unknown
Audio	Duration of music	Music in ad videos reduces irritation towards the ad.	Pelsmacker & Van den Bergh 1999	Positive
	Rapid speech	Rapid speech is associated with being more knowledgeable and an increase in watch time. Change in pace of influencer's voice grabs viewer attention.	Peterson et al. 1995; Guo et al. 2014 Beck 2015; Jennings 2021	Unknown
Images: Video Frames	Size of humans	Human images increase desire to socialize, engage and communicate.	Bakshi et al. 2014; Hartmann et al. 2021; To & Patrick 2021	Positive
	Size of packaged goods	Packshots (which focus on a product and not humans) decrease desire to socialize, engage and communicate.	Hartmann et al. 2021	Negative
	Size of animals	Ads featuring animals are more likeable.	Biel & Bridgwater 1990; Pelsmacker & Van den Bergh 1999	Positive
	Emotional expressions of joy and surprise	Joy and surprise in internet videos ads concentrate attention and retain viewers for longer periods of time. Joyous faces are associated with decrease in retweets but are not associated with likes on Twitter or Instagram. Surprise exhibited by instructors in educational videos has no dominant directional effect on video watch time, as it depends on contextual factors and topics discussed	Teixeira et al. 2012 Li & Xie 2020 Zhou et al. 2021	Unknown

Table 1: Theory-based stimuli and expectations

attention which can affect engagement with the video. Brand mentions (in captions/transcript) in influencer videos are stimuli that can lower entertainment value and increase informational value as discussion surrounding brand disclosure is typically commercial in nature (Tellis et al., 2019). This in turn can lead to a reduction in the persuasiveness of the message (Teixeira et al., 2010; Tellis et al., 2019), which can manifest as a reduction in (positive) sentiment for the video. On the other hand, a competing view suggests that increase in informational value may complement the entertainment value of video

content, educate viewers about the brand and increase viewers' trust in the brand (Leung et al., 2022; Lou & Yuan, 2019). This can be associated with an increase in (positive) sentiment for the video.

Use of emotional words has been found to be positively associated with engagement measures such as number of shares, comments and likes for Facebook ad messages or New York Times articles (Berger & Milkman, 2012; Lee et al., 2018). This is because emotional words are typically tied to a brand's personality and help increase persuasiveness of the message (Lee et al., 2018). Such words can also evoke high arousal leading to an excitatory state (Berger & Milkman, 2012). Hence, emotional words can be associated with an increase in (positive) sentiment for the video. A competing view suggests that use of emotional words is often associated with disingenuous persuasion or insincerity which is commonly found in fake news stories (Bakir & McStay, 2018; Guo et al., 2019). This would suggest that use of emotional words can be associated with a decrease in (positive) sentiment for influencer videos.

Given these contrasting set of findings in prior literature on the effect of brands and emotional words, their association with the sentiment for influencer videos is unclear ex-ante.

3.3.2 Duration of audio elements

Music in ad videos has been found to reduce irritation towards the ad (Pelsmacker & Van den Bergh, 1999) and correlate strongly with attitude shift (Haley et al., 1984). Furthermore, use of music without voiceover has been found to have a stronger effect than use of music with voiceover on memory for brand names (Alexomanolaki et al., 2007). Hence, an increase in the duration of music without voiceover can be expected to be associated with an increase in (positive) sentiment for the video.

Past research has found that fast speakers are rated as being more knowledgeable and more effective salespersons than slow speakers (Miller et al., 1976; Peterson et al., 1995). Similarly, research on educational videos has found that faster speaking rate of instructors is associated with an increase in watch time (Guo et al., 2014). On the other hand, linguists who have analyzed influencer videos find that a change in pace, and not rapid speech, is what grabs viewer attention (Beck, 2015; Jennings, 2021). This is not necessarily surprising given that one of the primary goals of influencers is to "entertain" viewers (Landsberg, 2021) which is further complemented with sales pitches or brand promotions. Given these contrasting results in prior research, it is unclear whether rapid speech can be expected to have a positive, negative or neutral association with sentiment for influencer videos.

3.3.3 Size of image elements

Human faces have been preferred in print ads (Xiao & Ding, 2014) and they have been associated with an increase in likes, comments and shares on social media posts (Bakhshi et al., 2014; Li & Xie, 2020; Yang et al., 2021). The reason for this positive association can be explained by the desire to socialize, engage and communicate with other humans (Bakhshi et al., 2014; To & Patrick, 2021). Moreover, in influencer

videos, the influencer is often demonstrating something to a viewer with the help of their hands, such as the details of a product. We expect this action of the influencer to further aid in engaging the viewer, and improve sentiment for the video. In summary, we can expect the size of the whole human (influencer) in the video, including the area near their hands, to be associated with an increase in (positive) sentiment.

Similarly, Hartmann et al. (2021) find that images of brand selfies and packshots are associated with a decrease in likes on Instagram as compared to consumer selfies because of a decrease in desire to engage with non-human images. Importantly, in influencer videos, packaged goods are objects that can draw attention in the video since influencers use them as part of a demonstration (e.g., unboxing video, tutorial, etc.). Hence, we expect an increase in size of packaged goods to have a negative association with the sentiment of engagement. Furthermore, just like videos featuring humans, ads featuring animals have been found to be more likeable and have an extremely low irritation score (Biel & Bridgwater, 1990; Pelsmacker & Van den Bergh, 1999). Hence, we expect an increase in size of animals in influencer videos to also be associated with an increase in (positive) sentiment for the video.

Facial expressions such as joy and surprise in internet video ads have been found to concentrate attention and retain viewers for longer periods of time (Teixeira et al., 2012). On the other hand, joyous (happy) faces have been found to be associated with fewer retweets on Twitter, and have been found to have *no* significant association with likes on Twitter or Instagram (Li & Xie, 2020). Similarly, surprise exhibited by instructors in educational videos has been found to either increase or decrease the likelihood of video watch time as its effect varies based on contextual factors and topics discussed (Zhou et al., 2021). Given these set of contrasting results on the effect of facial expressions, there is uncertainty about their association with the sentiment towards influencer videos.

We explain our process to extract these stimuli from text, audio and images in Section 6.1.

4. Data

We focus on influencer videos on YouTube, the platform where influencers charge the most for a post due to the higher production cost of long-form videos (Klear, 2019; McClure, 2020). This is the dominant form of content on YouTube as compared to other platforms such as TikTok, Instagram, Facebook, Twitter and Snapchat, which typically have short videos or image/text only posts (McClure, 2020). Such long-form videos are different from conventional ad videos in at least three ways (a) they can (and almost always do) contain information unrelated to the sponsoring brand (e.g., gaming videos, vlogs, etc.) (b) are much longer than a standard 30 sec TV ad, and (c) can be interrupted by traditional ads on YouTube.

4.1 Video Sample

We focus on 110 influencers identified by Forbes in February 2017 (O'Connor, 2017). Specifically, we look at 10 influencers in each of 11 product categories (Beauty, Entertainment, Fashion, Fitness, Food,

Gaming, Home, Parenting, Pets, Tech & Business, Travel). These influencers² are the top performers in their category, obtain revenue from brand endorsements and post mostly in English across Facebook, YouTube, Instagram and Twitter. In order to create our final data sample, we first exclude influencers who do not have a YouTube channel. We also use the industry threshold of 1000 followers for a person to be classified an influencer (Maheshwari, 2018) and also exclude one atypical influencer with more than 100M followers. Furthermore, we short-list those influencers who have posted at least 50 videos so that we can capture sufficient variation in their activity, which leaves us with a pool of 73 influencers.

Our selection criteria allow us to focus on popular YouTube influencers who primarily make content for adults, have between 1000 and 100M subscribers which is typical of the range of subscribership for influencers on YouTube, and posted only pre-recorded videos till November 2019. From this pool, we randomly choose 3 influencers per category, which gives a total of 33 influencers and a master list of 32,246 videos, whose title and posting time were scraped using the YouTube Data API v3 in October 2019³. From this pool of 33 influencers, we randomly choose 50 public videos for each influencer so that we have a balanced sample of 1650 videos whose unstructured data (text, audio and images) is computationally feasible to analyze in a reasonable amount of time (details in Section 7.1). Excluding videos in which likes, dislikes or comments were disabled by the influencer(s) leaves us with 1620 videos (all scraped in November 2019). Table 2 shows the specific data scraped.

Structured Data	Metrics	Number of views (from time of posting to time of scraping)
		Number of comments including replies (from time of posting to time of scraping)
		Number of likes (from time of posting to time of scraping)
		Number of dislikes (from time of posting to time of scraping)
	Length	Video Length (min)
	Tags	Tags associated with each video (see Google (2020) for details)
	Playlist	Number of playlists the video is a part of
		Position of video in each playlist
Number of videos on all the playlists the video is a part of		
Time	Time of posting video	
Unstructured Data	Text	Title, Description, Captions (if present)
		Comments (Top 25 as per YouTube’s proprietary algorithm) with replies
	Audio	Audio file
	Images	Thumbnail and Video File

Table 2: Scraped data for videos

4.2 Outcome Variables

The top three ways of measuring influencer marketing success in the industry are conversions, engagement and impressions (Influencer Marketing Hub, 2022). Unfortunately, conversion data are not

² The criteria used by Forbes to identify these influencers include total reach, propensity for virality, level of engagement, endorsements, and related offline business.

³ Our usage of this data falls within the ambit of YouTube’s fair use policy (YouTube, 2020).

publicly available, and the measure of impressions (views) can be confounded by the impact of YouTube's recommendation algorithm (explained ahead). Hence, we focus on engagement, which is important to brands to not only measure campaign success but also to ex-ante decide on a collaboration (Influencer Marketing Hub, 2022). Furthermore, measures of engagement (such as number of comments, likes, and sentiment of comments) have been linked with sales and profitability in related contexts such as brand managed social media communities (Goh et al., 2013; Gomez, 2021; Rishika et al., 2013).

We construct our measures of engagement using the dual-system framework – System I and System II – theory of human thinking (Dhar & Gorlin, 2013; Kahneman, 2003; Rottenstreich et al., 2007).⁴ System I thinking corresponds to more automatic and intuitive reactions that require less thought. This is captured by measures of shallow engagement that include a count of thumbs up / like (YouTube, Facebook, Instagram, etc.), thumbs down / dislike (YouTube and TikTok) or retweets (Twitter) that require little effort and can be accomplished with a simple click of a button (Social Media Week, 2017). System II thinking captures more effortful, conscious and deliberate reactions that require more thought. This is captured by measures of deep engagement that include a count of comments (YouTube, Facebook, Instagram, Twitter, etc.) which require more effort as it involves typing a response (Dwoskin, 2021).

Extant literature in marketing or extant metrics in the industry have typically not distinguished between measures of shallow or deep engagement likely because these measures are always highly correlated (Gogolan, 2022; Hartmann et al., 2021; Hughes et al., 2019; Lee et al., 2018). For example, across our sample of 1620 videos there is high correlation between log views and log (comments+1) at 0.91, between log views and log (likes+1) at 0.95 and between log views and log (dislikes+1) at 0.92 (we add 1 to avoid log of 0). An added concern in social media platforms is the confound of the recommendation algorithm that may be correlated with these measures of engagement. For example, YouTube's algorithm analyzes watch history and video content to recommend videos with higher expected watch time for a viewer, which should be highly correlated with total views for the video (Covington et al., 2016). We overcome the two problems of (1) high correlation between measures of shallow and deep engagement and (2) the confound of the YouTube algorithm, in the following manner. We construct engagement measures that control for the number of views, and hence capture shallow or deep engagement *conditional on viewing a video*. This results in unique constructs that are not highly correlated with each other or with views and are also dominated by distinct underlying factors (see 4.2.3). The absence of high correlation with views indicates that our measures are unlikely to be confounded by the algorithm. Similarly, any promotional activities by brands to increase the reach of influencer videos will result in an increase in views, but will not affect our measures of engagement.

⁴ These frames of thinking have also been introduced in prior research in related contexts such as peripheral and central routes of persuasion (Petty & Cacioppo, 1986) and heuristic and systematic modes of information processing (Chen & Chaiken, 1999).

We next explain our engagement measures through the prism of engagement level and the corresponding sentiment of engagement.

4.2.1 Engagement Level

We develop unique measures to capture the shallow and deep engagement level: (a) “Thumbsability”:
 $\frac{\#likes + \#dislikes}{\#views}$, which measures the level of shallow engagement and (b) “Commentability”:
 $\frac{\#comments}{\#views}$, which measures the level of deep engagement. Thumbsability is a measure of the number of thumbs up (likes) or thumbs down (dislikes) conditional on viewing the video.⁵ As this requires less thought and can be accomplished with a simple click (Social Media Week, 2017), it captures more automatic, intuitive and less deliberate reactions. On the other hand, commentability is a measure of number of comments conditional on viewing the video. As typing a response is more effortful and requires more thought (Dwoskin, 2021), this measure captures more conscious and deliberate reactions. By scaling each engagement measure by a count of views, we develop unique constructs that are not highly correlated with each other (see 4.2.3). As the two measures of engagement level are exponentially distributed, we take their natural log, and add 1 to avoid computation of log (0): log thumbsability = $\log\left(\frac{\#likes + \#dislikes + 1}{\#views}\right)$, and log commentability = $\log\left(\frac{\#comments + 1}{\#views}\right)$. Log thumbsability has a median of -3.78 (or approximately 228 likes or dislikes per 10K views) and log commentability has a median of -6.21 (or approximately 20 comments per 10K views).

4.2.2 Sentiment of Engagement

Past work has found that the visual and verbal components of advertising can have an effect on attitude towards the ad which in turn can have a direct effect on overall brand attitude, including attitude towards purchasing and using the product (Mitchell, 1986). Moreover, the sentiment of user generated content on brand managed social media communities has also been linked with sales (Goh et al., 2013). Hence, it is likely that brands would benefit from understanding viewer attitude or sentiment towards videos as it can act as a proxy for sales. We develop unique measures to capture the sentiment of shallow and deep engagement: (a) “Likeability”:
 $\frac{\#likes}{\#dislikes}$, which measures the sentiment of shallow engagement and (b) “Loveability”:
which measures the sentiment of deep engagement by capturing the sentiment in comments using Google’s Natural Language API.

Likeability measures the probability of a viewer to like rather than dislike a video. Higher the value of likeability, more positive is the sentiment of shallow engagement. As the measure is a ratio of two different measures, it is not highly correlated with the other outcome variables (see 4.2.3). As done

⁵ Note that from Nov 2021 YouTube has made thumbs down (dislike) counts private (<https://blog.youtube/news-and-events/update-to-youtube/>).

previously, we take the log of likeability and add 1 to avoid computation of $\log(0)$ or $\log(\infty)$: \log likeability = $\log\left(\frac{\text{likes}+1}{\text{dislikes}+1}\right)$. Log likeability has a median of 3.99 (or approximately 54 likes per dislike).

We capture loveability by measuring the average sentiment expressed in the Top 25 comments below a video. Note that comments below a video are by default sorted as ‘Top comments’ and not ‘Newest first,’ using YouTube’s proprietary ranking algorithm.⁶ We do not measure the sentiment in the replies to each of the Top 25 comments because sentiment expressed in the reply is likely to be sentiment towards the comment and not sentiment towards the video. We capture the sentiment in comments using Google’s Natural Language API which is pre-trained on a large document corpus, supports 10 languages, and is known to perform well in sentiment analysis on textual data (including emojis) in general use cases (Hopf, 2020; Li & Xie, 2020). For comments made in a language not supported by the API, we use the Google Translation API to first translate the comment to English, and then find its sentiment. The sentiment provided is a score from -1 to $+1$ (with increments of 0.1), where -1 is very negative, 0 is neutral and $+1$ is very positive. We calculate the sentiment of each comment below a video for a maximum of Top 25 comments, and then find the average sentiment score. As a robustness check, we use Top 50 or 100 comments for a random sample of 66 videos (2 videos per influencer) and also explore use of progressively decreasing weights instead of a simple average. We find that the sentiment calculated using any of these measures is highly correlated with a simple average of Top 25 comments ($\rho \geq 0.88$).

We use the median value (0.34) of the distribution of average sentiment score as a cut-off to divide loveability into two buckets – “positive” and “not positive (neutral or negative).” We convert loveability into a discrete measure instead of retaining a continuous measure because sentiment cannot be measured objectively using a continuous measure. There can be minor variations based on the choice of the API (or algorithm/human coder). Hence, by using a discrete measure, we are able to create a more objective measure of sentiment in comments, which is consistent with the approach used in prior research (Goh et al., 2013; Li & Xie, 2020). We also assume that if viewers choose to not post comments below a video (though comment posting is not disabled), then the sentiment towards the video is neutral.

4.2.3 Summary of outcome variables

We have a total of three continuous outcomes and one binary outcome that are summarized in Table 3a. We find that the average magnitude of the Pearson correlation coefficient between each of the four outcome variables is 0.28, with the individual values shown in Table 3b. This indicates that the measures on average are not highly correlated with each other.

⁶ Higher ranked comments (lower magnitude) have been empirically observed to be positively correlated with like/dislike ratio of comment, like/dislike ratio of commenter, number of replies to the comment and time since comment was posted (Dixon & Baig, 2019). Moreover, a tabulation shows that 99% of comments are made by viewers and not the influencer (who owns the channel) and hence we do not separate the two.

	Deep Engagement	Shallow Engagement
Engagement Level	Commentability: $\frac{\#comments}{\#views}$	Thumbsability: $\frac{\#likes+\#dislikes}{\#views}$
Sentiment of Engagement	Loveability: Positive or Not Positive	Likeability: $\frac{\#likes}{\#dislikes}$

Table 3a: Summary of outcome variables

	Log thumbsability	Log commentability	Log likeability	Loveability	Log views
Log thumbsability	1				
Log commentability	0.67	1			
Log likeability	0.53	0.14	1		
Loveability	0.01	-0.15	0.15	1	
Log views	0.18	0.04	0.43	-0.21	1

Table 3b: Correlation between variables

More importantly, we also carry out a Principal Component Analysis (PCA) on our outcome measures, as shown in Table 3c, and find that each measure loads heavily (≥ 0.83) on a distinct underlying construct. This provides further evidence that each outcome variable is capturing unique information: {deep or shallow} x {engagement level or sentiment}.

	Factor 1	Factor 2	Factor 3	Factor 4	Factor 5
Log thumbsability	0.45	0.32	0.07	0.02	0.83
Log commentability	0.96	0.04	0.00	-0.09	0.28
Log likeability	0.05	0.94	0.24	0.10	0.23
Loveability	-0.07	0.08	-0.11	0.99	0.01
Log views	0.01	0.21	0.97	-0.12	0.05

Table 3c: Factor Loadings from a PCA of variables

4.3 Ex-ante Features

Next, we generate features from the data scraped in Table 2, which are supplied *ex-ante* as input to our models in Section 5. We list these features in Table 4, and they can be divided into structured and unstructured features. Structured features comprise fixed effects for the influencer (channel), video length, number of tags, features for playlist information, time-based-features and an indicator for whether captions are available for the video. Unstructured features comprise text, audio and images. Text data comprise the title of the video, description below the video and captions/transcript of the video. For the video description, a maximum of 160 characters are visible in Google Search and even fewer characters are visible below the video before the ‘Show More’ link (Cournoyer, 2014). Hence, we truncate each description to the first 160 characters (160 c) as it is more likely to contribute to any potential association

with our outcomes. Captions are only present in 74% of videos, and for those videos without a caption, we use Google’s Cloud Speech-to-Text Video Transcribing API to transcribe the audio file to English.

Type	Class	Features	
Structured Features	Fixed Effects	Influencer Fixed Effects (33)	
	Length	Video Length (min)	
	Tags	Number of video tags	
	Playlist Information		Number of playlists the video is a part of
			Average position in playlist
			Average number of videos on all the playlists the video is a part of
	Time based covariates		Time between upload: Upload time and scrape time
			Year of upload (2006 to 2019)
			Time between upload: Given video and preceding video of influencer based on the master list
			Time between upload: Given video and succeeding video of influencer based on the master list
		Rank of video among all videos of the influencer in the master list	
		Day fixed effects (7) in EST and Time of day fixed effects in intervals of 4 hours from 00:00 hours EST (6)	
	Captions Indicator	Indicator of whether video has closed captions	
Unstructured features	Text	Title	
		Description (first 160 characters)	
		Captions or Transcript (beginning 30 sec, middle 30 sec and end 30 sec)	
	Audio	Audio file (beginning 30 sec, middle 30 sec and end 30 sec)	
	Images	Thumbnail	
Video Frames (beginning 30 sec, middle 30 sec and end 30 sec) at 1 frame per second			
Structured features from unstructured data	Complete Description	Total number of URLs in description	
		Indicator of Hashtag in description	

Table 4: Ex-ante video features - structured and unstructured

For the unstructured features of captions/transcript, audio and video frames, we focus on 30 seconds of data in the beginning, middle and end of the video for two reasons. First, the minimum duration of video content that needs to be viewed for an impression to be registered is 30 seconds (Parsons, 2017) which makes this an adequate threshold. Second, higher computational costs associated with analyzing *unstructured data* in our deep learning models require us to restrict data size to a feasible amount (e.g., it takes 432 hours to analyze images in our sample – details in Section 7.1). We use audio data in addition to captions/transcript to capture acoustics and analyze the presence and duration of sound elements such as music and human sounds. Image data comprise thumbnail and image frames captured at the conventional sampling frequency of one fps (frame per second) (Yang et al., 2021; Yue-Hei Ng et al., 2015) in 30 seconds of the beginning, middle and end of a video (i.e. 30 frames in each part of a video). These frames are at a good resolution of 135x240 pixels that is both visually clear and feasible to analyze.

Of the above unstructured features, the title, description (first 160c) and thumbnail image can be considered as “incentive to click” features, since they are visible in search results and prompt the viewer

to click on a video. We create two additional structured features from the complete description (as it is not supplied to the Text Model). These features are included as they can lead the viewer away from the video. They comprise total number of URLs in description and an indicator for hashtag in description.

We also check whether influencers comply with the US Federal Trade Commission (FTC) guidelines to disclose sponsorship early in the video using words such as “ad”, “sponsor”, etc. (FTC, 2020). We examine the captions/transcript in the beginning (and middle) of the video for such words and find that only 1% of videos make such disclosures which suggests little compliance with the guideline.

5. Model

We discuss our choice of the individual deep learning models (for text, audio and images) that benefit from transfer learning in 5.1. We then describe how we combine information from all models in 5.2.

5.1 Individual Models

We analyze text data using Bidirectional Encoder Representation from Transformers (BERT) (Devlin et al., 2018), a high performing NLP model that borrows the Encoder representation from the Transformer framework (Vaswani et al., 2017). The model is pre-trained using Book Corpus data (800M words) and English Wikipedia (2,500M words) to predict words and sentences over four days using four Tensor Processing Units. We fine-tune the BERT model on our data sample to capture the association with our four outcomes. We provide details on how we operationalize this framework in Online Appendix A.

The three main advantages of BERT over conventional deep learning models used in the marketing literature such as LSTM, CNN and CNN-LSTM that use word embeddings such as Glove and word2vec are as follows: (1) BERT learns contextual embeddings (e.g., the embedding for the word ‘bark’ will change based on the context in which it used – a dog’s bark or tree’s outer layer) (2) The entire BERT model with hierarchical layers is pre-trained whereas conventional models only initialize the first layer with a word embedding (3) BERT uses a *self-attention* mechanism that allows the model to simultaneously (non-directionally) identify importance (attention weights) associated with all words in text instead of using a sequential process that can lead to loss of information. We interpret these attention weights during ex-post interpretation in Section 6.

We analyze audio data using the pre-trained YAMNet model (Pilakal & Ellis, 2020), and customize it with an additional Bidirectional LSTM (Bi-LSTM) layer and an attention mechanism. YAMNet converts the raw audio signal into a Mel-frequency spectrogram (that captures the acoustic characteristics) of the audio signal. It then passes it through a MobileNet v1 model which is pre-trained on the AudioSet data (which has more than 2M 10-second YouTube audio segments) (Gemmeke et al., 2017). The Bi-LSTM layer helps capture the sequential interdependence between moments of sounds.

The attention mechanism, which we adopt from the literature on neural machine translation (Bahdanau et al., 2014), helps the Bi-LSTM model capture the relative importance (attention) weights between sound moments in order to form an association with an outcome. We interpret these attention weights during ex-post interpretation in Section 6. We provide details on how we operationalize this framework in Online Appendix B. Overall, the design of our model framework is novel, with a transfer learned MobileNet v1 architecture and an attention mechanism that help with both prediction and interpretation (Section 7).

We analyze individual images using the high performing and popular image model – VGG-16 that has been pre-trained on 1.2M images from ImageNet (Hartmann et al., 2021; Simonyan & Zisserman, 2014; Zhang et al., 2021). For analyzing video frames, we combine the output from each VGG-16 model with a Bi-LSTM, which is known to be one of the best performing architectures at capturing sequential information from video frames (c.f. Yue-Hei Ng et al. (2015)). We ex-post identify the salient areas of images that are associated with an outcome through gradient-based activation maps (cf. Selvaraju et al., 2017) and modify this such that positive (negative) gradients corresponding to regions that are positively (negatively) associated with continuous outcomes and the predicted class of the binary outcome. We provide details on how we operationalize the model and find gradients in Online Appendix C, and we analyze these gradients during ex-post interpretation in Section 6. While negative gradients identify areas that are negatively associated with an outcome, negative attention weights in the Text and Audio model identified areas that do not have an association. Note that we do not use an “attention weight” based approach here to find salient areas because that would be computationally very expensive over a 135x240 pixel frame for 30 frames. The gradient approach accomplishes the same objective more efficiently.

5.2 Combined Model

We use equation (1) to combine information from the unstructured and structured features. Information from the unstructured features is included by using the predicted outcome values \hat{Y}_{it} for video t by influencer i generated by supplying each unstructured feature (listed earlier in Table 4) to the appropriate individual model discussed in 5.1. The structured features, X_{it} , (listed earlier in Table 4) are supplied as an additional input to the equation. We test different models, g , to combine information from all these sources of data and capture any potential interactions between them. Equation (1) is shown below,

$$Y_{it} = g \left(\begin{array}{c} X_{it}, \hat{Y}_{it}^{Title}, \hat{Y}_{it}^{Description (first 160 c)}, \\ \hat{Y}_{it}^{Captions-Transcript (beginning)}, \hat{Y}_{it}^{Captions-Transcript (middle)}, \hat{Y}_{it}^{Captions-Transcript (end)}, \\ \hat{Y}_{it}^{Audio (beginning)}, \hat{Y}_{it}^{Audio (middle)}, \hat{Y}_{it}^{Audio (end)}, \\ \hat{Y}_{it}^{Thumbnail}, \\ \hat{Y}_{it}^{Video Frames (beginning)}, \hat{Y}_{it}^{Video Frames (middle)}, \hat{Y}_{it}^{Video Frames (end)} \end{array} \right) + \epsilon_{it} \quad (1)$$

where Y_{it} is the observed outcome for video t by influencer i , g is the combined model used and ϵ_{it} is the error term. We test the performance of seven different combined models that are known to predict well

out-of-sample. They comprise four linear models – OLS, Ridge Regression, LASSO and Elastic Net, and three non-linear models – Deep Neural Net, Random Forests and Extreme Gradient Boosting. Our choice of these combined models is guided by their high predictive performance in machine learning literature.

Note that we do not simultaneously train unstructured text, audio and image data (along with structured features) due to the extremely high computational (and monetary) cost⁷ associated with such an undertaking. While such an approach could improve out-of-sample predictive ability, this is not our main objective. Our primary goal of interpreting the relationships captured by each independent deep learning model (Section 6 and 7.2) without compromising on the predictive ability of each model (Section 7.1) is accomplished by our “interpretable deep learning” framework. We also do not create a unified multi-view representation of different elements in a video using latent dimensions because that will not allow for interpretation of the importance attributed to stimuli (which lie in the original dimension).⁸ We explain our approach towards interpretation in Section 6.

6. Interpretation Approach

We detail the implementation of our interpretation approach discussed earlier in Section 3.2 and Figure 2. First, we describe in 6.1 our process to generate the ex-post features that we use as the stimuli (discussed in 3.3) of interest. In 6.2, we detail Step 1 of our interpretation approach that uses the importance measures estimated from the individual models. Finally, in 6.3, we discuss Step 2 of our interpretation approach that uses the outcome values predicted by the individual models.

6.1 Ex-post Features

We generate ex-post features using trusted databases, reliable transfer learned models and accurate APIs, which is more efficient as compared to employing human coders. We elaborate on this below.

For text data, as discussed in 3.3.1, we focus on the following stimuli: presence of brand mentions and emotional words in captions/transcript⁹ in 30 seconds of the beginning, middle and end of a video. We identify these stimuli by applying *regular expressions* on textual data while relying on a master list of words. The master list of brand names comprise the Top 100 Global brands in 2019 that were obtained from BrandZ, Fortune100 and Interbrand. We then add more than 32,000 brands (with US offices) from the Winmo database to this list. This is further combined with brand names identified by applying Google’s Vision API - Brand Logo Detection on thumbnails and video frames (one fps in 30 seconds of beginning, middle and end) in our sample. From this combined list, we remove more than 800 generic

⁷ The analysis of our Image model alone has a high cost as it takes 432 hours to run (see details in Section 7.1).

⁸ Note that a Multi-Task Learning (MTL) approach to simultaneously predict all four outcomes will also not be suitable here because one of our primary goals is to interpret the relationship between theory-based stimuli and *each* engagement measure independently.

⁹ We do not study stimuli in features that are visible in search engine results such as title or description (and thumbnail), because they are visible before a video starts playing and hence help promote views. Our engagement measures, on the other hand, control for the number of views.

brand names such as ‘Slice,’ ‘Basic,’ ‘Promise,’ etc. that are likely to be used in non-brand related contexts. The master list of emotional words is obtained from the list of 2,469 emotional words identified in the LIWC dictionary (Berger & Milkman, 2012; Pennebaker et al., 2015). We identify brand and emotion mentions within 305,554 word-pieces that are generated by the BERT model using captions/transcript across all parts (beginning, middle and end) of the 1620 videos in our sample. We find that 28% (80%) of videos have a brand (emotion) mentioned at least once (in any part of the video).

For audio data, as discussed in 3.3.2, we mainly focus on the following stimuli: music and human speech in 30 seconds of the beginning, middle and end of a video. The YAMNet model (Mel Spectrogram + MobileNet v1) finds the predicted probability of each moment¹⁰ of a 30 second audio clip (which has 60 moments) belonging to a sound class. Our model can efficiently accomplish this identification for 291,600 moments (1620 videos x 3 parts x 60 moments in a part). We combine the identified sound classes into different categories based on the AudioSet ontology (Gemmeke et al., 2017) – *Human* (86%), *Music* (83%), *Animal* (17%), and *Others* which include sounds of silence, things, ambiguous sounds, background sounds and natural sounds. The percentage in brackets indicates the percentage of videos that contain a sound of that category (with probability > 0.5) in any part of the video. Note that a moment of sound can be classified into multiple categories if sounds from more than one category occur together.

For image data, as discussed in 3.3.3, we focus on the following stimuli: size of humans, size of face of humans, size of packaged goods, size of animals, and human facial expressions of joy and surprise. In addition, we also study the role of brand logos, and control for the size of everyday objects such as clothes & accessories and home & kitchen items. We study these stimuli in 30 frames that lie in 30 seconds of the beginning, middle and end of a video. We identify these stimuli using the Cloud Vision API from Google, that has been pre-trained on millions of images and whose high accuracy has been validated in prior academic and industry research (FileStack, 2019; Li & Xie, 2020; Szegedy et al., 2016). We can efficiently implement this API over 145,800 frames (1620 video x 3 parts of video x 30 frames per part). The API returns the vertices of the identified object which allows us to create a rectangular bounding box to define its area. We divide the identified objects into eight different categories – *Humans* (91%), *Faces* (86%), *Animals* (27%), *Brand Logos* (16%), *Packaged Goods* (28%), *Clothes & Accessories* (86%), *Home & Kitchen* (58%), and *Other Objects*. The percentage in brackets indicate the percentage of videos that contain an object of that category (in any part of the video).

6.2 Interpreting Relationship with Importance (Step 1)

After finding the estimated attention weights from the Text model for each word-piece in captions/transcript, we implement Step 1 of the interpretation approach 12 times by analyzing the

¹⁰ Each moment is 960ms long, and the subsequent moment begins after a hop of 490ms. Hence, each 30 second audio clip encompasses 60 moments. See details in Online Appendix B.

following equation for each outcome (four outcomes) and each 30 second part of the video – beginning, middle and end (three parts):

$$\log(\text{AttentionWeight}_{itk}) = \alpha_i + \gamma X_{it} + \sum_{k=1}^{n_b} \beta_{1k}(\text{BIT}_{itk}) + \sum_{k=1}^{n_e} \beta_{2k}(\text{EIT}_{itk}) + \beta_3(\text{TP}_{itk}) + \beta_4(\text{NOT}_{it}) + \epsilon_{itk} \quad (2)$$

where, $\text{AttentionWeight}_{itk}$ is the estimated weight for each token k (word-piece created from raw text by the model) in video t made by influencer i , α_i is influencer fixed effects, X_{it} is the same vector of structured features used earlier in equation (1). BIT_{itk} is ‘brand indicator in token’ indicating whether token k is a brand name, EIT_{itk} is ‘emotion indicator in token’ indicating whether token k is an emotional word, TP_{itk} is token k ’s position in the text, NOT_{it} is number of tokens in the text, n_b is total number of brands, n_e is total number of emotional words, and ϵ_{itk} is the error. We use a unique coefficient for each brand and emotional word to model potential heterogeneity in effects. We use a covariate for the token position (TP_{itk}) to control for any potential influence of the position of the word-piece in the text, and we control for the number of tokens (NOT_{it}) because attention weights in text are relative to each other and sum up to one, i.e. more the number of tokens, lower will be the attention directed to it.

Note that we cannot simultaneously control for presence of stimuli in all parts of the video in the same equation in Step 1 because the number of observations (e.g., tokens k) in each part of the video may be different (see Table 7 and Table 9 in Section 7.2 for the difference in number of observations).

After finding the estimated attention weights for each sound moment from the Audio model, we implement Step 1 of the interpretation approach 12 times by analyzing the following equation for each outcome (four outcomes) and each 30 second part of the video – beginning, middle and end (three parts):

$$\log(\text{AttentionWeight}_{itk}) = \alpha_i + \gamma X_{it} + \beta_1(\text{CI}(\text{Human})_{itk}) + \beta_2(\text{CI}(\text{Music})_{itk}) + \beta_3(\text{CI}(\text{Human})_{itk} \times \text{CI}(\text{Music})_{itk}) + \beta_4(\text{CI}(\text{Animal})_{itk}) + \beta_5(\text{CI}(\text{Other})_{itk}) + \beta_6(\text{Location}_{itk}) + \epsilon_{itk} \quad (3)$$

where, $\text{AttentionWeight}_{itk}$ is the estimated weight for moment k in video t made by influencer i , α_i is influencer fixed effects, X_{it} is the same vector of structured features used earlier in equation (1), $\text{CI}(\text{Human})$ is the Category Indicator for human sounds in moment k , and $\text{CI}(\text{Human}) \times \text{CI}(\text{Music})$ corresponds to moments when both human and music sounds occur together, Location_{itk} corresponds to location of the moment within 60 moments of the audio clip, and ϵ_{itk} is the error. We use a covariate for the location so that we can control for any potential influence of the position of the moment. Note that we do not include a covariate for number of audio moments, as each clip has the same length of 30 seconds.

After finding the estimated gradient values from the Image model, we implement Step 1 of the interpretation approach 12 times by analyzing the following equation for each outcome (four outcomes) and each 30 second part of the video – beginning, middle and end (three parts):

$$\begin{aligned}
MeanGradientValues_{itk} = & \alpha_i + \gamma X_{it} + \sum_{k=1}^8 \beta_{1k} SizeObject(k)_{it} + \beta_{21} Joy(Face)_{itk} + \\
& \beta_{22} Surprise(Face)_{it} + \beta_{23} Joy(Face)_{it} \times SizeObject(Face)_{it} + \\
& \beta_{24} Surprise(Face)_{it} \times SizeObject(Face)_{it} + \epsilon_{itk}
\end{aligned} \tag{4}$$

where, $MeanGradientValues_{itk}$ is the mean gradient values across the area (pixels) occupied by all items of object category k across 30 frames in video t made by influencer i , α_i is influencer fixed effects, X_{it} is the same vector of structured features used earlier in equation (1), and $k = 1$ to 8 corresponds to each object category: {humans, faces, animals, brand logos, packaged good, clothes & accessories, home & kitchen and other objects}. $SizeObject(k)_{it}$ is the mean across 30 frames of the percentage of the image occupied by all objects of category k in video t made by influencer i . Hence, the coefficient β_{1k} can be interpreted as the effect of a one percent increase in size of the object of category k on average across 30 seconds of the video. Note that features for size of humans and size of faces are not highly correlated (variance inflation factor ≤ 2.5 across each video part). $Joy(Face)_{it}$ and $Surprise(Face)_{it}$ indicate the mean (across 30 frames) of the level of surprise or joy in each face {-2: very unlikely, -1: unlikely, 0: possible, 1: likely, 2: very likely} as returned by the API. The two interaction terms capture the interaction between the emotion registered and the size of faces, and ϵ_{itk} is the error.

6.3 Interpreting Relationship with Outcome (Step 2)

After finding predicted outcome values from each of the Text, Audio and Image models we implement Step 2 of the interpretation approach 36 times by analyzing the following equation for each outcome and each part of a video {3 models x 4 outcomes x 3 parts of video }:

$$\begin{aligned}
PredictedOutcome_{it} = & \alpha_i + \gamma X_{it} + \sum_{p \text{ in part}} \{ \sum_{k=1}^{n_b} \beta_{1pk} (BITX_{it}) + \sum_{k=1}^{n_e} \beta_{2pk} (EITX_{it}) + \\
& \beta_{3p} (NOT_{it}) + \beta_{4p} (Sum \text{ of } CI(Human)_{it}) + \beta_{5p} (Sum \text{ of } CI(Music)_{it}) + \\
& \beta_{6p} (Sum \text{ of } CI(Human)_{it} \times Sum \text{ of } CI(Music)_{it}) + \beta_{7p} (Sum \text{ of } CI(Animal)_{it}) + \\
& \beta_{8p} (Sum \text{ of } CI(Other)_{it}) + \sum_{k=1}^8 \beta_{9pk} SizeObject(k)_{it} + \beta_{10p} Joy(Face)_{it} + \\
& \beta_{11p} Surprise(Face)_{it} + \beta_{12p} (Joy(Face)_{it} \times SizeObject(Face)_{it}) + \\
& \beta_{13p} (Surprise(Face)_{it} \times SizeObject(Face)_{it}) \} + \epsilon_{it}
\end{aligned} \tag{5}$$

where, $PredictedOutcome_{it}$ is a predicted outcome from a model for a part of video t made by influencer i , α_i is influencer fixed effects and X_{it} is the same vector of structured features used earlier in equation (1). $BITX_{it}$ is a ‘brand indicator in text’ indicating whether the text (captions/transcript) in video t by influencer i has a brand, $EITX_{it}$ is ‘emotion indicator in text’ indicating whether the text has an emotional word, and NOT_{it} is number of tokens in the text. As done in equation (2), we use a unique coefficient for each brand and emotional word to model potential heterogeneity in effects. We control for the number of tokens (NOT_{it}) to control for the potential influence of the length of the text on the outcome variable. $Sum \text{ of } CI(Human)_{it}$ corresponds to the duration of human sounds (or sum of the

Category Indicator for human sounds) across the 30 seconds (60 moments) in video t made by influencer i , and $Sum\ of\ CI(Human)_{it} \times CI(Music)_{it}$ finds the total duration when human and music sounds occur together. As we have controlled for the number of tokens (word-pieces), an increase in $Sum\ of\ CI(Human)_{it}$ can be interpreted as slower speech whereas a decrease in $Sum\ of\ CI(Human)_{it}$ can be interpreted as rapid speech. The other variables are identical to those used in equation (4). In summary, we control for stimuli across all sources of unstructured data (that were used earlier in the three equations of Step 1). We also sum over the $parts = \{beginning, middle, end\}$ of the video in equation (5) to control for the presence of words, sounds and objects in different locations of the video.

The values of the coefficients corresponding to each stimulus across Step 1 (Eq 2, 3 or 4) and Step 2 (Eq 5) will inform us whether the stimulus has a strong correlation with the predicted outcome (Step 2) that is also supported by an increase in importance attributed to the stimulus (Step 1).

7. Results

In this section, we first discuss the results of prediction in 7.1 and then interpretation in 7.2.

7.1 Prediction Results

We divide our random sample of 1620 videos into a random 60% training sample (972 videos), 20% validation sample (324 videos) and 20% holdout sample (324 videos) to estimate all our models.

7.1.1 Individual Models

We train the model on the training sample, tune the number of steps of Adam gradient descent on the validation sample, and then compute predictive performance on the holdout sample. Our parameter choices during model training are guided by the standard values used in the BERT, YAMNet and VGG-16 models (Devlin et al., 2018; Pilakal & Ellis, 2020; Simonyan & Zisserman, 2014). Importantly, we implement a form of bootstrapping, by repeating model training, validation and prediction 50 times (25 times) for every covariate-outcome pair in the Text and Audio models (Image Model) to mitigate concerns of model brittleness. This can be an issue if our models converge to different (local) optima in every instance of model training due to sensitivity to starting values of *hyperparameter* weights randomly chosen by our deep learning models.¹¹

We compare the predictive performance of our models with other standard benchmark models used in the marketing literature to demonstrate that our interpretable models do not compromise on predictive ability. We show the detailed results of predictive performance in Online Appendix D, and

¹¹ We carry out our analysis using one NVIDIA RTX A6000 GPU (48GB RAM) that takes the maximum time to analyze the Image model. For 25 bootstrap iterations, it takes around 36 hours to run the model and complete the gradient analysis for each covariate-outcome pair (e.g. beginning 30 sec-loveability). It takes a total of 432 hours {36 hours x 4 outcomes x 3 video parts} to analyze all covariate-outcome pairs. Hence, for computational ease, we restrict the number of iterations to 25 for the Image model, but go up till 50 iterations for the Text and Audio models.

summarize the key results here. We find that our Text model (BERT) has better prediction error than benchmarks such as LSTM, CNN (Liu et al., 2019), CNN-LSTM (Chakraborty et al., 2022) and CNN-Bi-LSTM. This demonstrates the benefit of a model that captures contextual word embeddings, has hierarchical layers and a self-attention mechanism as discussed earlier in Section 5.1. The Audio model has better prediction error than benchmarks that do not use the attention mechanism or MobileNet v1. This demonstrates that addition of transfer learning (through MobileNet v1) and the attention mechanism not only help with interpretability but also contribute towards the predictive ability of the Audio model. The Image model (VGG-16) has better prediction error than a conventional 4-layer CNN on thumbnail images, thus demonstrating the benefit of transfer learning and a deeper architecture. The Image model that is appended with a Bi-LSTM architecture to capture sequential information in video frames has better prediction error on average than an architecture that captures only spatial information. This demonstrates that sequential information in influencer videos is on average more important than spatial information in predicting engagement measures. Overall, we demonstrate that our interpretable models perform better than (i.e., have better prediction error), or at least as well as, other standard predictive models and thus we do not compromise on predictive ability (details in Online Appendix D). Table 5 summarizes the prediction errors from our models, for each component of unstructured data, and for each of the four outcome measures of engagement.

		Deep Engagement		Shallow Engagement	
		Sentiment	Engagement level	Sentiment	Engagement level
Model	Unstructured data	Loveability	Commentability	Likeability	Thumbsability
Text Model (BERT)	Title	0.72	0.68	0.71	0.47
	Description (first 160c)	0.70	0.77	0.89	0.51
	Captions/transcript (begin 30s)	0.71	0.85	0.96	0.56
	Captions/transcript (middle 30s)	0.69	0.96	1.05	0.62
	Captions/transcript (end 30s)	0.67	0.96	1.05	0.61
Audio Model (YAMNet + Bi-LSTM + Attention)	Audio (begin 30s)	0.64	0.86	1.03	0.63
	Audio (middle 30s)	0.63	0.91	1.04	0.64
	Audio (end 30s)	0.65	0.92	1.02	0.63
Image Model (VGG-16)	Thumbnail	0.68	0.93	1.01	0.61
Image Model (VGG-16 + Bi-LSTM)	Video Frames (begin 30s @1fps)	0.66	0.84	0.98	0.59
	Video Frames (middle 30s @1fps)	0.66	0.92	0.99	0.60
	Video Frames (end 30s @1fps)	0.67	0.89	0.96	0.57

Table 5: Model performance for each component of unstructured data in holdout sample (RMSE for Commentability, Thumbsability and Likeability; Accuracy for Loveability)

Our models predict all the continuous outcomes (commentability, thumbsability and likeability) with a RMSE ranging from 0.47 to 1.05 and the binary outcome (loveability) with accuracies ranging from 63% to 71%. For example, *captions/transcript in the beginning 30s* can be used to predict

commentability within an average RMSE range of $\pm e^{0.85} = \pm 2.4 \frac{\#comments+1}{\#views}$. Importantly, the sample standard deviation for the error and accuracy values across all the bootstrap iterations range from 0.01 to 0.06 across all our covariate-outcome pairs. The low value of the standard deviation demonstrates that our model iterations are quite stable. Of all the sources of unstructured data, the title of the video has the best out-of-sample predictive performance, which suggests that *title* is able to better discriminate between different influencers’ videos and/or within same influencers’ videos. We also find that the prediction error while using any of the unstructured components of captions/transcript, audio and video frames (in each part of the video) are close to each other while predicting all engagement measures. This suggests that when using these three unstructured components to make predictions, each of the three individual models (Text, Audio and Image) perform comparatively well in capturing variation in engagement.

7.1.2 Combined Model

To estimate the Combined Model in 5.2, we first re-predict each of our individual models in 5.1 on the entire sample (training, validation and holdout) to obtain \hat{Y}_{it} for video t by influencer i . We repeat this process for all bootstrap iterations and obtain the average of the predicted values. We then combine them with structured features X_{it} (as shown earlier in Eq (1)) using different combined models, g . We train each combined model on the training sample, validate the hyperparameters on the validation sample, and obtain predictions on the holdout sample. We find that Ridge Regression, a linear model, has the best performance on the holdout sample for all continuous outcomes (lowest RMSE) and the binary outcome (highest accuracy) as compared to OLS, LASSO, Elastic Net, Deep Neural Net, Random Forest and XGBoost (see Online Appendix D for details). This suggests that structured features and the predictions from individual models for unstructured data do not have substantial interactions with each other.

Now, the predicted outcomes from the individual models (\hat{Y}_{it}) supplied as features to the Combined Model can be collinear with each other. However, all features with multicollinearity in the Ridge Regression model are regularized equally towards the null, and hence their relative importance can be captured by the model. We measure relative importance of each feature by taking the magnitude of each estimated coefficient from the Ridge Regression model applied on the training sample and scale it by the sum of the magnitude of all coefficient values. This gives us the relative importance or percentage contribution of each feature while predicting each engagement measure.¹² This is shown in Table 6 (Panel A). Note that as the features used in the model (\hat{Y} in Eq 1) can be collinear with each other, the feature importance measures should be interpreted as conveying a combination of *between-influencer* (different influencer’s videos) and *within-influencer* (same influencer’s videos) importance of a measure.

¹² As we scale all the features by their $L2$ norm before running the model, the coefficients are regularized to the same degree and hence we can make relative comparisons. Also, we sum up the coefficient values that lie within a class (e.g., sum up coefficient values of influencer fixed effects, sum up other structured features (in Table 4)) to get an overall idea of the contribution of a class of features in predicting each outcome.

		Deep Engagement		Shallow Engagement	
		Sentiment	Engagement level	Sentiment	Engagement level
		Loveability	Comment-ability	Likeability	Thumbs-ability
Panel A					
Structured data					
Structured Features	Influencer Fixed Effects	18.0%	2.9%	31.8%	39.5%
	Other features (Table 4)	36.8%	2.4%	7.7%	10.5%
Total		54.8%	5.4%	39.4%	49.9%
Unstructured data					
Incentive to Click Features	Title	9.4%	25.4%	15.5%	9.9%
	Description (first 160c)	9.1%	22.7%	13.0%	7.6%
	Thumbnail	0.1%	2.6%	1.9%	2.2%
	Total	18.5%	50.8%	30.3%	19.7%
Captions / Transcript	Begin 30s	5.7%	13.7%	9.5%	7.1%
	Middle 30s	5.7%	10.7%	4.7%	5.6%
	End 30s	5.7%	7.4%	4.4%	5.5%
	Total	17.0%	31.7%	18.7%	18.2%
Audio	Begin 30s	1.1%	3.0%	1.0%	1.7%
	Middle 30s	0.8%	1.0%	1.2%	1.3%
	End 30s	0.7%	1.7%	1.7%	1.9%
	Total	2.6%	5.7%	3.8%	4.9%
Video Frames	Begin 30s	4.1%	3.0%	2.4%	2.4%
	Middle 30s	1.0%	1.2%	2.0%	2.1%
	End 30s	2.0%	2.4%	3.3%	2.6%
	Total	7.1%	6.5%	7.7%	7.1%
Panel B					
Total Begin 30s		10.9%	19.7%	12.9%	11.2%
Total Middle 30s		7.4%	12.8%	7.9%	9.1%
Total End 30s		8.4%	11.4%	9.4%	10.0%

Table 6: Importance of features based on the Combined Model

We find that influencer fixed effects are especially important for predicting measures of shallow engagement (39.5% for thumbsability and 31.8% for likeability). This suggests that characteristics unique to an influencer are important in predicting automatic reactions from viewers, but other structured and unstructured features are more important in predicting deeper engagement from viewers. While “incentive to click” features are more likely to drive a change in views than engagement by definition (as discussed earlier in Section 4.3), their power in explaining engagement with the video suggests correlation between them and the content of the video. This is especially prominent for title and description (first 160 characters) which explain more variation in all the engagement measures than thumbnail images do.

Importantly, we find that captions/transcript explain more than twice the variation in all engagement measures than audio or video frames across each part of the video (beginning, middle or end). This demonstrates that words spoken by the influencer are more influential in capturing variation in engagement than audio-visual features. From this we can conclude that “what is said” (words spoken) is

more important than “how it is said” (imagery and acoustics) to distinguish between engagement levels of different videos (by the same or different influencer). Furthermore, video frames across each part of the video explain more variation in all the engagement measures as compared to audio. This demonstrates that when deciding how to convey information, imagery (e.g., color of product, background objects, clothes worn, etc.) is more important than acoustics (e.g., voice intonation, background music, etc.). Note that these conclusions are possible because the Text, Image or Audio model predict comparatively well when using captions/transcript, video frames, or audio respectively (across each part of the video) as discussed earlier in 7.1.1. Hence these results may not be attributed to better predictive ability of one individual (unstructured) model as compared to the other.

These findings show that the substance of the message (in captions/transcript) conveyed by the influencer is more influential than the presentation choice in imagery (video frames) or acoustics (audio). This is consistent with the age-old advertising adage of Ogilvy – “*What you say is more important than how you say it: the information you give is more important to the consumer than the way you present it.*” (Ogilvy, 1983). Our findings are also novel to the broader advertising literature, as previous literature has not documented the relative influence of these three components (in ad videos) on marketing outcomes, to the best of our knowledge. While our findings are correlational, they provide general directions along which improvements are most likely. Hence, influencers are likely to benefit from prioritizing working on their choice of words, followed by the choice of imagery, and finally the choice of acoustics.

Next, we analyze the relative importance of features in each part of the video in Table 6 (Panel B). We find that, on average, unstructured features in the beginning of videos explain more variation in all the engagement measures than unstructured features in the middle or end of videos. This demonstrates that stimuli in the beginning are typically more salient than stimuli used later in videos, consistent with findings in prior research for ad videos (Tellis et al., 2019). Hence, influencers may focus more energy on designing the beginning of videos, than later parts of videos, to improve engagement.

7.2 Interpretation Results

We now detail the results of our ex-post interpretation approach. We estimate equation (2) (that interprets importance measures from the Text model) using Ridge Regression to capture heterogeneity in effects across brands and emotional words. Similarly, we estimate equation (5) using Ridge Regression when modeling the predicted outcomes from the Text model (and present additional reasons for our modelling choice in Online Appendix E). We estimate equations (3) and (4) (that interpret importance measures from the Audio and Image models) using OLS. Similarly, we estimate equation (5) using OLS when modeling the predicted outcomes from the Audio or Image models (see details in Online Appendix E).

We interpret the results of ex-post interpretation on the entire sample of 1620 videos by re-predicting each of our deep learning models on the entire sample to take advantage of complete

information in our data. Note that our interpretation is carried out for each bootstrap iteration (mentioned earlier in Section 7.1), that is repeated 50 times (25 times) for every covariate-outcome pair in Text and Audio models (Image Model), to mitigate potential concerns of brittleness as discussed earlier in 7.1. Our robustness checks in Section 7.2.4 provide further validation for the results obtained using our approach.

7.2.1 Interpretation Results for Text Model

As mentioned above, we estimate equations (2) (Step 1) and (5) (Step 2) using Ridge Regression to capture heterogeneity in effects. In order to obtain the ridge parameter, we train equation (2) on the training sample over a wide array of ridge parameters, then validate it on the validation sample to obtain the ridge parameter that minimizes loss. We then use this ridge parameter and estimate equation (2) over the entire sample of videos to take advantage of complete information in our data.

We present the results of the analysis for brand and emotion mentions in Table 7. The table displays the percentage of total brands and percentage of total emotional words that have a positive and/or negative predictive effect on attention weights (Eq 1) and predicted outcome (Eq 5). We represent a positive effect with a + sign and negative effect with a - sign. However, when calculating this percentage, we ignore brands/emotions whose value is less than 5% of the magnitude of the maximum predictive effect on the respective outcome in Eq (1) or (5). We use this *threshold* of 5% (robustness discussed ahead) so that we can ignore non-important predictors whose coefficients have been shrunk towards 0 by the Ridge Regression model. We can draw two main conclusions from the table. First, Step 1 of our analysis shows that brands and emotional words are salient as they are paid more attention to than not. This is because the % of mentions which capture positive attention is higher than the percentage of mentions which capture negative attention in either the beginning, middle or end of videos. Thus, Step 1 of our interpretation approach allows us to filter out non-important brands and emotional words, and focus our analysis on important mentions. Second, using Step 2 of our interpretation approach we find that the important brand and emotion mentions more often have a negative association when predicting loveability (deep engagement), and more often have a positive association when predicting likeability (shallow engagement). We also show a graphical visualization of Table 7 in Online Appendix E.

Moreover, for the beginning 30 seconds, the difference between the percentage of brands that have a positive vs negative (predictive) effect on the predicted outcome continue to hold true across a range of values of the *threshold* used in Table 7 (see details in Online Appendix E). In other words, we demonstrate how our findings for the beginning 30s are robust to brands/emotions that have a small or a large effect on the engagement measures.¹³ We highlight in grey the corresponding cells with dominant effects in Table 7. Also, as per theory, we do not expect any association between use of brands or

¹³ Note that the results for loveability are also robust for the middle and end of video which is not surprising because Table 6 showed that captions/transcript in each video part are equally important in predicting loveability but the beginning is more important for predicting likeability.

emotional words in the beginning 30 seconds and measures of commentability and thumbsability. Our results also do not show evidence of a robust association.

	(Eq 1) Attention Weights (Step 1)	(Eq 5) Predicted Outcome (Step 2)	Sentiment of Engagement			
			Brands		Emotions	
			Deep	Shallow	Deep	Shallow
			Loveability	Likeability	Loveability	Likeability
Beginning	+	+	21.6%	38.6%	8.3%	29.0%
	+	-	42.5%	29.4%	23.3%	19.5%
	-	+	0.7%	2.0%	8.1%	10.7%
	-	-	4.6%	3.3%	11.1%	10.6%
Middle	+	+	20.0%	26.4%	11.4%	22.1%
	+	-	36.4%	21.8%	20.3%	16.5%
	-	+	8.2%	2.7%	10.9%	8.1%
	-	-	11.8%	7.3%	16.5%	7.3%
End	+	+	18.4%	33.3%	9.4%	20.3%
	+	-	40.2%	26.4%	20.5%	16.9%
	-	+	5.7%	5.7%	8.1%	11.5%
	-	-	3.4%	3.4%	13.0%	8.3%

Sample Size: N = 114,536 tokens in beginning 30s, 107,411 tokens in middle 30s, 83,607 tokens in end 30s (Step 1); N = 1620 videos (Step 2)
Threshold: 5% (% of max coefficient value used to ignore non-important predictors that have been shrunk towards 0 by Ridge Regression)

Table 7: Interpretation results of the Text model

Our findings for brand mentions suggest that a decrease in entertainment value resulting from a discussion of commercial content in the beginning may negatively affect deliberate reactions from some viewers which is captured by a reduction in loveability (Teixeira et al., 2010; Tellis et al., 2019). This is consistent with prior research that has found a decrease in sharing of commercial content on YouTube (Tellis et al., 2019). However, an increase in informational value associated with brand mentions in the beginning may positively affect automatic reactions from other viewers that is captured by an increase in likeability (Leung et al., 2022; Lou & Yuan, 2019). This is consistent with prior research that has found an increase in sharing of commercial content on Weibo (Leung et al., 2022). Hence, we find evidence for both of the competing hypotheses discussed earlier in 3.3.1. Notably, we find that the same category of brands – electronics and digital – are primarily associated with both a decrease in loveability and increase in likeability. Specifically, we find that 38% of brands that are associated with a decrease in loveability are also associated with an increase in likeability. While we do find heterogeneity in effects across 62% of brands, the overlap of 38% and the dominant effect of a specific category of brands suggests there also exists heterogeneity among viewers in their response to the same brand mentions.

Our findings for emotional words suggest that emotional word mentions in the beginning can have a positive effect on automatic and intuitive reactions from some viewers (captured by an increase in likeability). This is consistent with prior research that has found a positive effect of emotional words on number of shares, comments and likes for Facebook ad messages or New York Times articles (Berger &

Milkman, 2012; Lee et al., 2018). However, emotional word mentions in the beginning can also have a negative effect on deliberate reactions (captured by a decrease in loveability). This can arise because viewers may associate emotional words with disingenuous persuasion or insincerity which commonly occurs in fake news (Bakir & McStay, 2018; Guo et al., 2019). Hence, we find evidence for both of the competing hypotheses discussed earlier in 3.3.1. Notably, we find that both positively and negatively valenced emotional words (Pennebaker et al., 2015) are associated with the two relationships, suggesting that a difference in the valence of words is not driving the effects. We also find that 37% of emotional words that are associated with a decrease in loveability are also associated with an increase in likeability. While the difference of 63% suggests heterogeneity in effects across emotional words, an overlap of 37% suggests heterogeneity among viewers in their response to the use of same emotional words.

Importantly, for the previously discussed four associations (highlighted in grey in Table 7), we find that the average frequency (over 50 bootstrap iterations) with which a brand/emotional word (that meets the 5% threshold) continues to have the same directional (+/−) effect on attention and predicted outcome is very high (76% to 93%). This demonstrates that we are able to mitigate concerns of brittleness that can arise because of random model convergence to a local optimum during one iteration of training. By bootstrapping over 50 iterations, the brand/emotion coefficients tend to converge towards a dominant directional effect.

Overall, the heterogeneity in viewer response to the same brands and emotional words suggests that the same video content can activate the intuitive System I thinking in the minds of some viewers and the more deliberate System II thinking in the minds of other viewers (Kahneman, 2003). Some viewers may rely more on one of the two systems or the same stimuli may make activate different systems for different viewers (Dhar & Gorlin, 2013; Rottenstreich et al., 2007). System I thinking would make viewers respond more automatically and intuitively with the press of the like or dislike button. System II thinking would make viewers think about their reaction and then type a comment below the video. Viewers whose System I thinking is activated on being exposed to brand names or emotional words seem more likely to respond favorably with a quick like for the video, thus increasing likeability. On the other hand, viewers whose System II thinking is activated seem more likely to respond unfavorably (or neutrally) to the video in their comments, thus decreasing loveability.

7.2.2 Interpretation Results for Audio Model

We estimate equations (3) (Step 1) and (5) (Step 2) using OLS (for continuous outcomes) and logistic regression (for binary outcome) on the entire sample of videos. The results are shown in Table 8. The table shows the median value of coefficients, β , across 50 bootstrap iterations, where the coefficient value reflects a percent change in the (non-log-transformed) outcome when a sound moment is present (Eq 3) or

sound duration increases by one moment (Eq 5). The rows below each coefficient reflect the percentage of time (across 50 iterations) the corresponding p value is statistically significant. We highlight those cells in green that are significant at least 80% of the time across both Step 1 and 2. Our choice of the 80% threshold (as compared to a less conservative 50% (even chance) threshold) lends more confidence that these results are less likely to be spurious or confounded. Similarly, we highlight those cells in orange that are significant at least 80% of the time in only one of Step 1 or Step 2, and correspond to spurious or confounded relationships respectively.

		Deep Engagement						Shallow Engagement					
		Sentiment			Engagement level			Sentiment			Engagement level		
		Loveability			Commentability			Likeability			Thumbsability		
		Begin	Middle	End	Begin	Middle	End	Begin	Middle	End	Begin	Middle	End
Eq (3) Attention Weights (Step 1)	Human β_1	-3.9%	17.8%	-0.4%	2.6%	9.5%	0.0%	0.0%	24.7%	1.0%	0.0%	2.5%	9.4%
	p <= 0.05	49%	55%	58%	60%	86%	50%	56%	82%	50%	52%	78%	68%
	Music β_2	248.3%	78.8%	-0.6%	13.9%	4.7%	0.0%	0.0%	15.9%	0.1%	0.5%	3.3%	1.3%
	p <= 0.05	96%	63%	52%	92%	54%	74%	82%	60%	80%	82%	56%	64%
	H x M β_3	-54.4%	-46.0%	3.9%	-5.3%	-7.1%	0.0%	0.0%	-5.8%	0.0%	0.0%	-1.1%	0.0%
	p <= 0.05	90%	65%	64%	78%	82%	62%	68%	60%	72%	60%	58%	42%
	Animal β_4	354.3%	1325.2%	111.7%	0.0%	0.0%	0.0%	0.0%	52.5%	0.0%	0.0%	1.1%	10.1%
p <= 0.05	90%	80%	92%	46%	20%	78%	52%	68%	72%	38%	44%	68%	
Eq (5) Predicted Outcome (Step 2)	Human β_1	-2.5%	-6.5%	-4.6%	-0.2%	0.1%	-0.4%	0.2%	0.3%	0.3%	-0.1%	-0.1%	-0.4%
	p <= 0.05	29%	69%	46%	38%	48%	82%	78%	90%	74%	40%	52%	90%
	Music β_2	30.6%	20.5%	16.4%	-2.0%	-1.4%	-1.5%	-0.3%	0.0%	-0.2%	-0.9%	-0.7%	-1.1%
	p <= 0.05	100%	96%	96%	100%	100%	100%	78%	50%	70%	100%	100%	100%
	H x M β_3	-18.0%	-7.6%	-15.1%	-0.4%	0.2%	0.7%	0.1%	0.1%	0.0%	-0.1%	0.1%	0.4%
	p <= 0.05	82%	61%	64%	52%	52%	82%	58%	54%	24%	34%	66%	54%
	Animal β_4	51.5%	72.6%	98.0%	-0.1%	0.6%	1.6%	0.8%	1.2%	1.2%	-0.5%	0.7%	4.3%
p <= 0.05	59%	57%	84%	2%	38%	82%	90%	96%	76%	20%	74%	94%	

Sample Size: N = 97,200 moments in beginning 30s, middle 30s or end 30s (Step 1); N= 1620 videos (Step 2)
Highlighted green (orange) cells: p value is significant ≤ 0.05 at least 80% of the time across 50 iterations in both (only one of) Step 1 and Step 2

Table 8: Interpretation results of the Audio Model

We summarize a few of the key results corresponding to the cells in green. As can be seen in Table 8, an increase in duration of music (without simultaneous speech) by one moment (about half a second) within the beginning 30 seconds is associated with an increase in the odds ratio of loveability by 30.6% (Eq 5), but also a decrease in commentability by 2.0% (Eq 5). These associations are significant 100% of the time across our 50 iterations (Eq 5) and are also supported by a significant increase in attention at least 90% of the time (Eq 3). These effects are especially dominant in the beginning than in the middle or end of the video, as evidenced by the more frequent positive significant effects for attention (>90%) in the beginning (Eq 3) when the stimuli is new and more salient. However, the association between music in the first 30 seconds and measures of shallow engagement is weaker or significant less often, suggesting that music has a stronger association with measures of deep engagement than shallow engagement. The positive association between the duration of music and the sentiment of deep

engagement is consistent with our general expectation in 3.3.2 where we discussed the positive affective influence of music in advertising literature (Haley et al., 1984; Pelsmacker & Van den Bergh, 1999). In addition, our finding of a reduction in commentability suggests that there may also be a net reduction in the number of negative comments below the video, which could contribute to the increase in loveability. Overall, the strong association between music in the beginning and our measures of deep engagement suggests that music strongly influences deliberate reactions from viewers (System II thinking).

We also find no occasion where the coefficient for the duration of human sounds is *negative* in Step 2 and significant more than 80% of the time in both steps. This suggests that there is no strong association between *rapid* speech in any part of the video and our measures of engagement, consistent with the expectation of linguists who have analyzed influencer videos (Beck, 2015; Jennings, 2021). Note that a decrease in the duration of human sounds can be interpreted as rapid speech because we control for the number of word-pieces, as discussed earlier in Section 6.3. However, we do observe a positive association between *slower* speech (*positive* coefficient for duration of human sounds) in the middle 30 seconds and likeability, suggesting that the middle of the video maybe an important place to slow down.

Overall, as shown in Table 8, we exclude 5 spurious relationships (orange cells corresponding to Eq 3) that are only frequently significant in Step 1, and 13 confounded relationships (orange cells corresponding to Eq 5) that are only frequently significant in Step 2. By using a two-step process we identify a smaller subset of 6 relationships (green cells) at the intersection of Step 1 and Step 2.

7.2.3 Interpretation Results for Image Model

We estimate equations (4) and (5) using OLS (for continuous outcomes) and logistic regression (for binary outcome) on the entire video sample. The results are shown in Table 9. The table shows the median value of coefficients, β , across 25 bootstrap iterations, where the coefficient value reflects a percent change in the (non-log-transformed) outcome when size of an object increases by one percent on average across 30 video frames. The rows below each coefficient reflect the percentage of time (across 25 iterations) the corresponding p value is statistically significant. As done in 7.2.2, we highlight those cells in green (orange) that are significant at least 80% of the time across both (only one of) Step 1 and 2.

We summarize a few of the key results corresponding to the cells in green. An increase in size of human images by 1% in the beginning, middle or end of a video is associated with a 0.4%, 0.2% or 0.4% increase in likeability (sentiment of shallow engagement) respectively which is consistent with our expectations in 3.3.3. These associations are significant at least 90% of the time across our 25 iterations (Eq 5) and are also supported by a significant increase in attention 100% of the time (Eq 3). However, we do not find a corresponding positive association with the sentiment of deep engagement that is frequently significant across both Steps 1 and 2. This demonstrates that human images elicit automatic and intuitive reactions from viewers that can manifest easily as a like for the video. Furthermore, the association

between size of face and sentiment of shallow or deep engagement is not frequently significant. This demonstrates that the image of the entire human is more important, when controlling for the size of the face. This is reasonable because the size of the whole human will be correlated with the area of the screen where they are demonstrating something to the viewer with the help of their hands.

We also find evidence that an increase in size of packaged goods by 1% in the beginning 30 seconds is associated with a decrease in likeability (sentiment of shallow engagement) by 0.7%. Overall, both the previous findings for human images and packaged goods are consistent with Hartmann et al. (2021) who find that consumer selfies (i.e., human images) receive more likes than brand selfies and packshots (i.e., packaged goods) on Instagram. The desire to socialize, engage and communicate with other humans is likely driving these effects (Bakhshi et al., 2014; Hartmann et al., 2021; To & Patrick, 2021). Notably, our results are true for sentiment of shallow engagement but not sentiment of deep engagement suggesting that the desire for social interaction is manifested more easily in quick reactions.

		Deep Engagement						Shallow Engagement					
		Sentiment			Engagement level			Sentiment			Engagement level		
		Loveability			Commentability			Likeability			Thumbsability		
		Begin	Middle	End	Begin	Middle	End	Begin	Middle	End	Begin	Middle	End
Eq (4) Mean Gradients (Step 1)	Humans β_{11}	0.0%	0.0%	0.1%	0.8%	0.8%	0.9%	0.8%	0.8%	0.9%	0.9%	0.8%	0.9%
	p <= 0.05	100%	100%	96%	100%	100%	100%	100%	100%	100%	100%	100%	100%
	Faces β_{12}	-0.2%	-0.1%	-0.2%	0.8%	0.5%	0.3%	0.6%	0.4%	0.3%	1.0%	0.6%	0.2%
	p <= 0.05	56%	12%	60%	100%	96%	56%	100%	100%	60%	100%	100%	48%
	Animals β_{13}	0.2%	0.3%	0.3%	1.1%	1.1%	1.2%	1.2%	1.3%	1.4%	1.2%	1.2%	1.3%
	p <= 0.05	100%	100%	100%	100%	100%	100%	100%	100%	100%	100%	100%	100%
	B Logos β_{14}	0.0%	-0.1%	0.0%	0.1%	-0.2%	0.2%	-0.1%	-0.2%	0.0%	0.0%	-0.1%	0.1%
	p <= 0.05	0%	0%	0%	0%	0%	0%	0%	0%	0%	0%	0%	0%
	P Goods β_{15}	0.1%	-0.1%	0.0%	0.7%	0.7%	0.8%	0.7%	0.7%	0.6%	0.7%	0.5%	0.7%
p <= 0.05	0%	0%	0%	100%	96%	100%	100%	100%	96%	100%	92%	96%	
Eq (5) Predicted Outcome (Step 2)	Humans β_{11}	0.0%	1.5%	1.8%	0.3%	0.2%	0.0%	0.4%	0.2%	0.4%	0.4%	0.3%	0.1%
	p <= 0.05	8%	76%	60%	64%	52%	44%	92%	96%	92%	96%	96%	48%
	Faces β_{12}	7.4%	3.4%	3.3%	0.9%	0.0%	0.6%	0.4%	0.5%	-0.8%	0.9%	0.9%	0.4%
	p <= 0.05	48%	16%	12%	44%	48%	24%	0%	52%	32%	68%	96%	28%
	Animals β_{13}	5.3%	4.1%	13.3%	0.6%	0.0%	0.0%	1.0%	0.6%	1.7%	0.9%	0.4%	0.6%
	p <= 0.05	16%	4%	100%	56%	16%	36%	100%	88%	100%	96%	36%	88%
	B Logos β_{14}	8.6%	22.8%	1.6%	-0.6%	0.0%	0.8%	0.4%	-0.4%	-3.8%	0.3%	-1.2%	0.1%
	p <= 0.05	8%	8%	0%	0%	0%	4%	0%	0%	72%	0%	12%	4%
	P Goods β_{15}	-1.6%	-3.1%	-3.6%	-0.2%	0.0%	0.0%	-0.7%	0.0%	-0.3%	-0.5%	-0.2%	0.2%
p <= 0.05	8%	0%	8%	4%	28%	24%	88%	8%	12%	84%	0%	12%	

Sample Size: N = 5868 objects in beginning 30s, 5659 objects in middle 30s and 5519 objects in end 30s (Step 1); N = 1620 videos (Step 2)
Highlighted green (orange) cells: p value is significant ≤ 0.05 at least 80% of the time across 50 iterations in both (only one of) Step 1 and Step 2

Table 9: Interpretation results of the Image Model

We also find that an increase in size of animals by 1% in the beginning, middle or end of video is associated with a 1.0%, 0.6% or 1.7% increase in likeability respectively. This is consistent with our expectation as ads featuring animals have been found to be more likeable and have an extremely low irritation score (Biel & Bridgwater, 1990; Pelsmacker & Van den Bergh, 1999). We do not find frequent

significant associations between facial expressions of joy or surprise and our measures of engagement which is consistent with results found in related domains (Li & Xie, 2020; Zhou et al., 2021). It is important to note that inferences of emotion (made either by humans or NLP API’s) on facial expressions in images rely on commonly based heuristics and need not reflect the true emotion being experienced by the person (Barrett et al., 2019). This could be one of the main reasons for not observing significant effects. We also do not find frequent significant associations for everyday objects such as images of clothes & accessories and home & kitchen items. Hence, we do not report their coefficient values in Table 9. Overall, we identify 14 relationships (green cells) at the intersection of Step 1 and Step 2, and exclude 24 spurious relationships (orange cells corresponding to Eq 4) that are only frequently significant in Step 1. Note that we do not find confounded relationship in Step 2 that lie above the 80% threshold.

7.2.4 Summarizing Insights

We used a two-step process for identifying a subset of relationships between stimuli in text, audio or images and our measures of engagement. For interpreting the Text model, we first filtered out non-important brands and emotional words (Step 1) and then investigated whether important brands and emotional words more often have a positive or negative effect on our engagement measures (Step 2). For interpreting the Audio and Image model, we filtered out spurious relationships from Step 1 and confounded relationships from Step 2, and identified relationships at the intersection. The majority of our findings at the intersection correspond to the beginning 30 seconds of the video, which again demonstrates that stimuli in the beginning are more salient on average than stimuli in the middle or end of the video (consistent with our prediction-based findings in 7.1). We summarize these results (at the intersection) for the beginning 30 seconds in Table 10.

		Deep Engagement		Shallow Engagement	
		Sentiment	Engagement level	Sentiment	Engagement level
Unstructured Data	Stimuli	Loveability	Commentability	Likeability	Thumbsability
Text: Captions/ Transcript	Brand names	–		+	
	Emotional words	–		+	
Audio	Music	+	–		–
Images: Video Frames	Human			+	+
	Animal			+	+
	Packaged goods			–	–

Table 10: Summary of key interpretation results for the beginning 30 seconds

We show the direction of association between a stimulus and an outcome by a + or – sign. These relationships are obtained while controlling for stimuli across all sources of unstructured and structured data, and are hence unlikely to be confounded by observed video features. Furthermore, the grey cells in the table correspond to results that can be supported by theory discussed earlier in 3.3. As shown in Table

10, for the beginning 30 seconds, our stimuli in text have an association with *sentiment* of both deep and shallow engagement. However, our stimuli in audio have an association with *sentiment* of deep engagement while our stimuli in images have an association with *sentiment* of shallow engagement.

As discussed earlier in 4.3, our findings are unlikely to be affected by YouTube’s recommendation algorithm or a brand’s promotional activities to increase reach of a video, because “views” is not highly correlated with our measures of engagement. We also conduct two robustness checks to further validate our findings and interpretation approach. First, we carry out ex-post interpretation by estimating equation (5) on a random 80% sample of the 1620 videos, and find that all the substantive findings summarized in Table 10 continue to hold true with approximately the same effect sizes and frequency of significance as before. This demonstrates that our main results are not sensitive to the size of our chosen sample. Second, we carry out simulations to demonstrate that our models and ex-post interpretation approach is able to recover the true data generating process (see Online Appendix F). The results of our simulation provide external validity to our interpretable deep learning framework. While our interpretation approach is able to eliminate several spurious and confounded relationships (in Steps 1 and 2), it does not guarantee causality. However, the subset of relationships at the intersection can be validated by theory. They can be further validated in future work by formal causal testing in the field. Thus, our approach significantly reduces the effort required for future causal work.

8. Implications for Influencers and Marketers

In this section, we discuss how our interpretable deep learning framework and related findings can be useful for practitioners (influencers and marketers) in at least four possible ways.

First, our results in Section 7.1 demonstrate that influencers’ choice of words helps distinguish engagement levels more than imagery or acoustics. Our finding empowers influencers by providing them general directions along which to prioritize their efforts while designing videos. Changing their choice of words could be easier and more cost effective for influencers than changing imagery (e.g., shooting location, use of visual effects) or acoustics (e.g., quality of microphone and background music) in a video.

Second, brands that sponsor influencers can benefit from a clear understanding of how mentions across different types of brands are associated with engagement. As discussed earlier in 7.2.1, brand mentions are more often associated with an increase in likeability but a decrease in loveability. Both these associations are dominated by brands in the electronics and digital categories. Thus, brands in these categories may find it useful to rigorously investigate the level of tradeoff and determine whether the increase in likeability is worth the reduction in loveability. Similarly, packaged good brands maybe better off having their images displayed in the middle of the video than in the beginning where it is associated with a decrease in likeability. Hence, brands can use our results to modify their brand integration strategy

while still complying with the FTC guidelines discussed earlier in Section 4.3. Furthermore, our results summarized in Table 10 will help influencers identify video elements that can have a strong influence on engagement. They can focus their efforts towards fine-tuning specific elements in their videos and more rigorously test for changes in engagement measures. For example, influencers can experiment with increasing duration of background music (without voice-over) in the beginning of the video and test the corresponding increase in loveability.

Third, besides evaluating specific elements, marketers may also be interested in evaluating influencer videos in a holistic manner. We develop a video scoring mechanism to help them determine the influence of unstructured components in influencer videos. A video can be scored out of 100% on each of its unstructured elements when predicting any of the engagement measures. We do this with the help of the combined Ridge Regression model shown earlier in equation (1). We begin by creating a linear Partial Dependence Plot (PDP) (Friedman, 2001) between $\hat{Y}_{it<unstructured>}$ and Y_{it} in the training sample, where the value of $\hat{Y}_{it<unstructured>}$ is the average across all bootstrap iterations (as done earlier in Section 7.1). We note the values of $\hat{Y}_{it<unstructured>}$ that correspond to a minimum and a maximum change in the predicted outcome. We then note the values of $\hat{Y}_{it<unstructured>}$ for a random video in the holdout sample. We scale it using min-max scaling to get a score out of 100% for each unstructured element while predicting each outcome. Finally, we get an overall score by weighing the score for each unstructured element with its relative importance score (found earlier in Table 6 - Panel A).

As an illustration, let us take the point of view of a brand that is evaluating a particular influencer as a potential partner. As a sample, they pick this video (https://www.youtube.com/watch?v=3-oWqeA_hc4) and score it as above which is shown in Table 11. We can see that the video's weakest performance area based on its overall score is on both its engagement levels – commentability (30.6%) and thumbsability (48.5%) – and the corresponding weakest elements are captions/transcript in the beginning 30 seconds (10.1%) and audio in the middle 30 seconds (26.0%) respectively. Brands and agencies can use these scores to suggest areas of improvement to influencers, and compare scores of this video to scores from other videos of the same or a different influencer. These scores can be used in conjunction with the visualization techniques described in Online Appendix G to help influencers identify areas for improvement. Influencers can use these scores to progressively refine their videos for the relevant engagement measure that is of concern to them or the brand partner. Note that these summary scores are based on correlations between video elements and engagement, so their value lies in providing directions along which improvements are most likely. In contrast, without these scores, the number of directions on which influencers and brands can work is very large.

Fourth, a bigger question for marketers is to understand the overall importance of branded content in these influencer videos. One way to quantify this is to decompose the variance explained by brand

		Deep Engagement		Shallow Engagement	
		Sentiment	Engagement level	Sentiment	Engagement level
		Loveability	Commentability	Likeability	Thumbsability
Incentive to Click features	Title	100.0%	23.9%	75.1%	51.5%
	Description (first 160c)	100.0%	34.0%	73.5%	62.7%
	Thumbnail	0.0%	87.5%	46.3%	26.5%
Captions/ Transcript	Begin 30s	100.0%	10.1%	76.6%	44.0%
	Middle 30s	100.0%	25.7%	80.7%	50.5%
	End 30s	100.0%	24.2%	88.2%	50.5%
Audio	Begin 30s	0.0%	83.6%	48.9%	26.7%
	Middle 30s	0.0%	19.5%	72.9%	26.0%
	End 30s	100.0%	67.0%	57.6%	31.9%
Video Frames	Begin 30s	100.0%	45.2%	63.6%	62.7%
	Middle 30s	0.0%	23.0%	49.0%	28.6%
	End 30s	100.0%	60.9%	69.0%	59.2%
Overall Score		93.6%	30.6%	72.9%	48.5%
	Observed value for video	Positive	6 comments per 10K views	118 likes per dislike	181 likes or dislikes per 10K views

Table 11: Score for a random influencer video outside the training sample

related content in the relationship between a covariate-outcome pair. We decompose the variance explained by brand mentions in the relationship between captions/transcript in the beginning 30 seconds and likeability/loveability in Online Appendix G. We find that brand mentions explain 8.1% of the variance in likeability and perform 10% better than chance in predicting loveability. This demonstrates that brand mentions have a small but substantial role to play in explaining the behavior of both the sentiment of shallow and deep engagement. We also find that words other than brand names in captions/transcript (beginning 30 sec) explain more variation in loveability than likeability.

9. Conclusion

This paper adds to the small body of work on an important and growing marketing mechanism, influencer marketing. The main vehicle used in influencer marketing is influencer videos, with brands sponsoring and/or inserting advertising during these videos. There is virtually no research on how the constituent elements of these videos across text, audio and images are related to measures of shallow and deep engagement that both influencers and marketers care about. This paper takes the first step at documenting these relationships. More importantly, we develop a novel “interpretable deep learning” framework that solves the conventional challenge of making a tradeoff between interpretability and predictive ability. This is accomplished by carrying out ex-post interpretation on the same model that makes good out-of-sample predictions with unstructured data (text, audio, and images). First, our models use unstructured data across multiple modalities as input to predict engagement with the video, and then we combine information from all modalities to quantify the relative importance of structured and unstructured features

in predicting our engagement measures. This allows us to discover that “what is said” (captured by words in captions/transcript) is more important than “how it is said” (captured by acoustics in audio and imagery in video frames) in explaining engagement. However, when it comes to conveying information, imagery is more important than acoustics. Furthermore, we also find that stimuli in the beginning of videos are on average more salient than stimuli in the middle or end of videos.

After completing the prediction step, we then ex-post “peek” inside the model to interpret the captured relationships between theory-based stimuli and our measures of engagement. We accomplish this by adapting the attention capture and transfer framework in the advertising literature (Pieters & Wedel, 2004) to our influencer video setting. Our novel ex-post interpretation approach is implemented in two steps. First, we quantify the importance (attention weights or gradients) attributed to words in text, moments in audio and pixels in images, to study whether a change in the stimuli of interest is correlated with the importance attributed to them. Second, we study whether a change in the stimuli is correlated with the outcomes predicted by our models. By looking at relationships that fall at the intersection of both steps, we are able to filter out relationships that are affected by spuriousness due to peculiarities of deep learning models and confounding factors unassociated with importance attributed to the stimuli. Our key findings and interpretation approach are supported by theory and multiple robustness checks including simulations which show that we can recover the true data generating process. This significantly reduces the effort required for further work focused on uncovering causal relationships. Our interpretation-based findings can also be seen as consistent with prior work in related domains of video advertising and social media. However, they are also novel in their ability to distinguish between effects on shallow (System I) and deep (System II) engagement that are based on Kahneman’s theory of frames of human thinking. Moreover, a broader view suggests that our “interpretable deep learning” framework can also be adapted to the analysis of long-form videos across multiple domains e.g., entertainment, education and politics.

Given that the paper represents early work on the analysis of unstructured data in influencer videos, it suffers from some limitations. First, as we have no access to sales data from influencer campaigns, we use proxy metrics that, while relevant to marketers, may not be perfectly correlated to business metrics. Interestingly, however, brands find it very difficult to assess the ROI of influencer marketing campaigns, suggesting that measurement of sales data is non-trivial (Bailis, 2020; Kramer, 2018). Second, as our sample includes only influencers who use brand endorsements, we cannot offer any insights about the quality of videos from those influencers who never receive such endorsements. Third, the uncovered relationships between video stimuli and outcomes, while based on a two-step process that eliminates spurious and confounded relationships, do not guarantee causality. While these relationships can be validated by theory, their casual effects need to be confirmed, e.g., via field experiments. Fourth, while YouTube is one of the most important influencer marketing platforms for long-form videos, there

may be systematic differences in how influencer videos work on other channels (such as Instagram or TikTok) or newly launched platform extensions such as YouTube Shorts for short-form videos. Finally, our findings may vary by type of video (e.g., product reviews, unboxing videos, tutorials, etc.) or type of device (e.g., mobile, desktop and tablet) used to view a video, but our results only capture the average effect. We hope that future work can address these limitations.

Funding and Competing Interests

All authors certify that they have no affiliations with or involvement in any organization or entity with any financial interest or non-financial interest in the subject matter or materials discussed in this manuscript. The authors have no funding to report.

References

- Alexomanolaki, M., Loveday, C., & Kennett, C. (2007). Music and memory in advertising: Music as a device of implicit learning and recall. *Music, Sound, and the Moving Image*, 1(1), 51-72.
- Bahdanau, D., Cho, K., & Bengio, Y. (2014). Neural machine translation by jointly learning to align and translate. *arXiv preprint arXiv:1409.0473*.
- Bailis, R. (2020). The State of Influencer Marketing: 10 Influencer Marketing Statistics to Inform Where You Invest. <https://www.bigcommerce.com/blog/influencer-marketing-statistics/#what-is-influencer-marketing>
- Bakhshi, S., Shamma, D. A., & Gilbert, E. (2014). Faces engage us: Photos with faces attract more likes and comments on instagram. Proceedings of the SIGCHI conference on human factors in computing systems,
- Bakir, V., & McStay, A. (2018). Fake news and the economy of emotions: Problems, causes, solutions. *Digital journalism*, 6(2), 154-175.
- Barrett, L. F., Adolphs, R., Marsella, S., Martinez, A. M., & Pollak, S. D. (2019). Emotional expressions reconsidered: Challenges to inferring emotion from human facial movements. *Psychological science in the public interest*, 20(1), 1-68.
- Beck, J. (2015). *The Linguistics of 'YouTube Voice'*. Retrieved December 7 from <https://www.theatlantic.com/technology/archive/2015/12/the-linguistics-of-youtube-voice/418962/>
- Berger, J., & Milkman, K. L. (2012). What makes online content viral? *Journal of Marketing Research*, 49(2), 192-205.
- Biel, A. L., & Bridgwater, C. A. (1990). Attributes of likable television commercials. *Journal of Advertising Research*, 30(3), 38-44.
- Brooks, A. (2020, January 24). *As influencers increasingly create video content, what does this mean for brands?* <https://marketingtechnews.net/news/2020/jan/24/influencers-increasingly-create-video-content-what-does-mean-brands/>
- Burnap, A., Hauser, J. R., & Timoshenko, A. (2021). Design and Evaluation of Product Aesthetics: A Human-Machine Hybrid Approach. Available at SSRN 3421771.
- Chakraborty, I., Kim, M., & Sudhir, K. (2022). Attribute sentiment scoring with online text reviews: Accounting for language structure and missing attributes. *Journal of Marketing Research*, 59(3), 600-622.
- Chen, L., Yan, Y., & Smith, A. N. (2022). What drives digital engagement with sponsored videos? An investigation of video influencers' authenticity management strategies. *Journal of the Academy of Marketing Science*, 1-24.
- Chen, S., & Chaiken, S. (1999). The heuristic-systematic model in its broader context.
- Cheng, M. M., & Zhang, S. (2022). Reputation Burning: Analyzing the Impact of Brand Sponsorship on Social Influencers. Working Paper, Available on SSRN: https://papers.ssrn.com/sol3/papers.cfm?abstract_id=4071188.
- Cournoyer, B. (2014, March 19). *YouTube SEO Best Practices: Titles and Descriptions*. <https://www.brainshark.com/ideas-blog/2014/March/youtube-seo-best-practices-titles-descriptions>

- Covington, P., Adams, J., & Sargin, E. (2016). Deep neural networks for youtube recommendations. Proceedings of the 10th ACM conference on recommender systems,
- Devlin, J., Chang, M.-W., Lee, K., & Toutanova, K. (2018). Bert: Pre-training of deep bidirectional transformers for language understanding. *arXiv preprint arXiv:1810.04805*.
- Dew, R., Ansari, A., & Toubia, O. (2022). Letting logos speak: Leveraging multiview representation learning for data-driven branding and logo design. *Marketing Science*, 41(2), 401-425.
- Dhar, R., & Gorlin, M. (2013). A dual-system framework to understand preference construction processes in choice. *Journal of Consumer Psychology*, 23(4), 528-542.
- Dixon, C., & Baig, H. (2019, March 7). *What is Youtube comment system sorting / ranking algorithm?* . <https://stackoverflow.com/questions/27781751/what-is-youtube-comment-system-sorting-ranking-algorithm>
- Dwoskin, J. (2021). *There's A Big Difference Between Likes and Comments*. Retrieved June 5 from <https://www.stampede.social/there-s-a-big-difference-between-likes-and-comments>
- Dzyabura, D., El Kihal, S., & Ibragimov, M. (2022). Leveraging the power of images in managing product return rates. Available at SSRN: <https://ssrn.com/abstract=3209307> or <http://dx.doi.org/10.2139/ssrn.3209307>.
- Dzyabura, D., & Yoganarasimhan, H. (2018). Machine learning and marketing. In *Handbook of Marketing Analytics*. Edward Elgar Publishing.
- FileStack. (2019). *Comparing Image Tagging Services: Google Vision, Microsoft Cognitive Services, Amazon Rekognition and Clarifai*. Retrieved April 25 from <https://blog.filestack.com/thoughts-and-knowledge/comparing-google-vision-microsoft-cognitive-amazon-rekognition-clarifai/>
- Friedman, J. (2001). Greedy function approximation: a gradient boosting machine. *Annals of statistics*, 1189-1232.
- FTC. (2020). *Disclosures 101 for Social Media Influencers*. https://www.ftc.gov/system/files/documents/plain-language/1001a-influencer-guide-508_1.pdf
- Gemmeke, J. F., Ellis, D. P., Freedman, D., Jansen, A., Lawrence, W., Moore, R. C., Plakal, M., & Ritter, M. (2017). Audio set: An ontology and human-labeled dataset for audio events. 2017 IEEE International Conference on Acoustics, Speech and Signal Processing (ICASSP),
- Gogolan, D. (2022). *Engagement Rate for All Social Media Platforms*. Retrieved January 11 from <https://www.socialinsider.io/blog/engagement-rate/>
- Goh, K.-Y., Heng, C.-S., & Lin, Z. (2013). Social media brand community and consumer behavior: Quantifying the relative impact of user-and marketer-generated content. *Information systems research*, 24(1), 88-107.
- Gomez, R. (2021). *8 ways customers interact and engage with your brand on social*. Retrieved May 19 from <https://sproutsocial.com/insights/social-media-interaction/>
- Google. (2016). *Consumer Insights*. <https://www.thinkwithgoogle.com/consumer-insights/consumer-trends/top-reasons-viewers-watch-youtube/>
- Google. (2020). *Add tags to videos*. <https://support.google.com/youtube/answer/146402?hl=en>
- Guo, C., Cao, J., Zhang, X., Shu, K., & Yu, M. (2019). Exploiting emotions for fake news detection on social media. *arXiv preprint arXiv:1903.01728*.
- Guo, P. J., Kim, J., & Rubin, R. (2014). How video production affects student engagement: An empirical study of MOOC videos. Proceedings of the first ACM conference on Learning@ scale conference,
- Haley, R. I., Richardson, J., & Baldwin, B. M. (1984). The effects of nonverbal communications in television advertising. *Journal of Advertising Research*, 24(4), 11-18.
- Hartmann, J., Heitmann, M., Schamp, C., & Netzer, O. (2021). The power of brand selfies. *Journal of Marketing Research*, 58(6), 1159-1177.
- Hopf, M. (2020). *NLP With Google Cloud Natural Language API*. <https://www.toptal.com/machine-learning/google-nlp-tutorial>
- Huang, Y., & Morozov, I. (2022). Video Advertising by Twitch Influencers. Available at SSRN 4065064.
- Hughes, C., Swaminathan, V., & Brooks, G. (2019). Driving Brand Engagement Through Online Social Influencers: An Empirical Investigation of Sponsored Blogging Campaigns. *Journal of Marketing*.
- Hwang, S., Liu, X., & Srinivasan, K. (2021). Voice Analytics of Online Influencers—Soft Selling in Branded Videos. *Working Paper*, Available at SSRN 3773825.
- Influencer Marketing Hub. (2022). *The State of Influencer Marketing*. https://influencermarketinghub.com/ebooks/Influencer_Marketing_Benchmark_Report_2022.pdf
- Jennings, R. (2021). *How should an influencer sound?* Retrieved July 13 from <https://www.vox.com/the-goods/2021/7/13/22570476/youtube-voice-tiktok-influencer-sound>
- Kahneman, D. (2003). Maps of bounded rationality: Psychology for behavioral economics. *American economic review*, 93(5), 1449-1475.

- Klear. (2019). *Influencer Marketing Rate Card*. <https://klear.com/KlearRateCard.pdf>
- Kramer, S. (2018, September 4). *The Impact of Influencer Marketing on Consumers*. <https://www.themarketingscope.com/influencer-marketing-on-consumers/>
- Landsberg, N. (2021). *60 Powerful Video Marketing Statistics*. <https://influencermarketinghub.com/video-marketing-statistics/>
- Lanz, A., Goldenberg, J., Shapira, D., & Stahl, F. (2019). Climb or Jump: Status-Based Seeding in User-Generated Content Networks. *Journal of Marketing Research*, 56(3), 361-378.
- Lee, D., Hosanagar, K., & Nair, H. S. (2018). Advertising content and consumer engagement on social media: Evidence from Facebook. *Management Science*, 64(11), 5105-5131.
- Lee, D., Manzoor, E., & Cheng, Z. (2022). Focused Concept Miner (FCM): An Interpretable Deep Learning for Text Exploration. Available at SSRN: <https://ssrn.com/abstract=3304756>
- Leung, F. F., Gu, F. F., Li, Y., Zhang, J. Z., & Palmatier, R. W. (2022). EXPRESS: Influencer Marketing Effectiveness. *Journal of Marketing*, 00222429221102889.
- Li, X., Shi, M., & Wang, X. S. (2019). Video mining: Measuring visual information using automatic methods. *International Journal of Research in Marketing*, 36(2), 216-231.
- Li, Y., & Xie, Y. (2020). Is a picture worth a thousand words? An empirical study of image content and social media engagement. *Journal of Marketing Research*, 57(1), 1-19.
- Liu, L., Dzyabura, D., & Mizik, N. (2020). Visual listening in: Extracting brand image portrayed on social media. *Marketing Science*, 39(4), 669-686.
- Liu, X., Lee, D., & Srinivasan, K. (2019). Large-scale cross-category analysis of consumer review content on sales conversion leveraging deep learning. *Journal of Marketing Research*, 56(6), 918-943.
- Lou, C., & Yuan, S. (2019). Influencer marketing: how message value and credibility affect consumer trust of branded content on social media. *Journal of Interactive Advertising*, 19(1), 58-73.
- Lu, S., Xiao, L., & Ding, M. (2016). A video-based automated recommender (VAR) system for garments. *Marketing Science*, 35(3), 484-510.
- Maheshwari, S. (2018, November 11). *Are You Ready for the Nanoinfluencers?* <https://www.nytimes.com/2018/11/11/business/media/nanoinfluencers-instagram-influencers.html>
- McClure, B. (2020). *How much do influencers charge per post?* <https://impact.com/partnerships/how-much-do-influencers-charge-per-post/>
- Miller, N., Maruyama, G., Beaver, R. J., & Valone, K. (1976). Speed of speech and persuasion. *Journal of personality and social psychology*, 34(4), 615.
- Mitchell, A. A. (1986). The effect of verbal and visual components of advertisements on brand attitudes and attitude toward the advertisement. *Journal of Consumer Research*, 13(1), 12-24.
- O'Connor, C. (2017, September 26). *Forbes Top Influencers: Meet The 30 Social Media Stars Of Fashion, Parenting And Pets (Yes, Pets)*. <https://www.forbes.com/sites/clareoconnor/2017/09/26/forbes-top-influencers-fashion-pets-parenting/>
- Ogilvy, D. (1983). *Confessions of an advertising man*. Atheneum New York.
- Parsons, J. (2017, August 24). *How Long Until Watching a YouTube Video Counts as a View?* <https://growtraffic.com/blog/2017/08/youtube-video-counts-view>
- Pei, A., & Mayzlin, D. (2022). Influencing social media influencers through affiliation. *Marketing Science*, 41(3), 593-615.
- Pelsmacker, P. D., & Van den Bergh, J. (1999). Advertising content and irritation: a study of 226 TV commercials. *Journal of international consumer marketing*, 10(4), 5-27.
- Pennebaker, J. W., Boyd, R. L., Jordan, K., & Blackburn, K. (2015). *The development and psychometric properties of LIWC2015*.
- Peterson, R. A., Cannito, M. P., & Brown, S. P. (1995). An exploratory investigation of voice characteristics and selling effectiveness. *Journal of Personal Selling & Sales Management*, 15(1), 1-15.
- Petty, R. E., & Cacioppo, J. T. (1986). The elaboration likelihood model of persuasion. In *Communication and persuasion* (pp. 1-24). Springer.
- Pieters, R., & Wedel, M. (2004). Attention capture and transfer in advertising: Brand, pictorial, and text-size effects. *Journal of Marketing*, 68(2), 36-50.
- Pilakal, M., & Ellis, D. (2020). *YAMNet*. <https://github.com/tensorflow/models/tree/master/research/audioset/yamnet>
- Rishika, R., Kumar, A., Janakiraman, R., & Bezawada, R. (2013). The effect of customers' social media participation on customer visit frequency and profitability: an empirical investigation. *Information systems research*, 24(1), 108-127.

- Rottenstreich, Y., Sood, S., & Brenner, L. (2007). Feeling and thinking in memory-based versus stimulus-based choices. *Journal of Consumer Research*, 33(4), 461-469.
- Selvaraju, R. R., Cogswell, M., Das, A., Vedantam, R., Parikh, D., & Batra, D. (2017). Grad-cam: Visual explanations from deep networks via gradient-based localization. Proceedings of the IEEE international conference on computer vision,
- Simonyan, K., & Zisserman, A. (2014). Very deep convolutional networks for large-scale image recognition. *arXiv preprint arXiv:1409.1556*.
- Social Media Week. (2017). *Social Media Metrics Compared: Which Are The Most Valuable?* Retrieved October 19 from <https://socialmediaweek.org/blog/2017/10/social-media-metrics-compared-valuable/>
- Statista. (2023). *Global Influencer Marketing Size from 2020 to 2025*. <https://www.statista.com/statistics/1328195/global-influencer-market-value/>
- Szegedy, C., Vanhoucke, V., Ioffe, S., Shlens, J., & Wojna, Z. (2016). Rethinking the inception architecture for computer vision. Proceedings of the IEEE conference on computer vision and pattern recognition,
- Teixeira, T., Wedel, M., & Pieters, R. (2010). Moment-to-moment optimal branding in TV commercials: Preventing avoidance by pulsing. *Marketing Science*, 29(5), 783-804.
- Teixeira, T., Wedel, M., & Pieters, R. (2012). Emotion-induced engagement in internet video advertisements. *Journal of Marketing Research*, 49(2), 144-159.
- Tellis, G. J., MacInnis, D. J., Tirunillai, S., & Zhang, Y. (2019). What drives virality (sharing) of online digital content? The critical role of information, emotion, and brand prominence. *Journal of Marketing*, 83(4), 1-20.
- Tian, Z., Dew, R., & Iyengar, R. (2022). Mega or Micro? Influencer Selection Using Follower Elasticity. *Working Paper*, Available on SSRN: https://papers.ssrn.com/sol3/papers.cfm?abstract_id=4173421.
- Timoshenko, A., & Hauser, J. R. (2019). Identifying customer needs from user-generated content. *Marketing Science*, 38(1), 1-20.
- To, R. N., & Patrick, V. M. (2021). How the eyes connect to the heart: The influence of eye gaze direction on advertising effectiveness. *Journal of Consumer Research*, 48(1), 123-146.
- Vashishth, S., Upadhyay, S., Tomar, G. S., & Faruqui, M. (2019). Attention interpretability across nlp tasks. *arXiv preprint arXiv:1909.11218*.
- Vaswani, A., Shazeer, N., Parmar, N., Uszkoreit, J., Jones, L., Gomez, A. N., Kaiser, Ł., & Polosukhin, I. (2017). Attention is all you need. *Advances in neural information processing systems*,
- Weiss, K., Khoshgoftaar, T. M., & Wang, D. (2016). A survey of transfer learning. *Journal of Big data*, 3(1), 1-40.
- Wiegrefe, S., & Pinter, Y. (2019). Attention is not not explanation. *arXiv preprint arXiv:1908.04626*.
- Wilbur, K. C. (2016). Advertising content and television advertising avoidance. *Journal of Media Economics*, 29(2), 51-72.
- Woltman Elpers, J. L., Wedel, M., & Pieters, R. G. (2003). Why Do Consumers Stop Viewing Television Commercials? Two Experiments on the Influence of Moment-to-Moment Entertainment and Information Value. *Journal of Marketing Research (JMR)*, 40(4).
- Xiao, L., & Ding, M. (2014). Just the faces: Exploring the effects of facial features in print advertising. *Marketing Science*, 33(3), 338-352.
- Yang, J., Zhang, J., & Zhang, Y. (2021). First law of motion: Influencer video advertising on tiktok. Available at SSRN 3815124.
- YouTube. (2020). *What is fair use?* <https://www.youtube.com/intl/en-GB/howyoutubeworks/policies/copyright/>
- Yue-Hei Ng, J., Hausknecht, M., Vijayanarasimhan, S., Vinyals, O., Monga, R., & Toderici, G. (2015). Beyond short snippets: Deep networks for video classification. *Proceedings of the IEEE conference on computer vision and pattern recognition*, 4694-4702.
- Zhang, M., & Luo, L. (2022). Can consumer-posted photos serve as a leading indicator of restaurant survival? Evidence from yelp. *Management Science*.
- Zhang, S., Lee, D., Singh, P. V., & Srinivasan, K. (2021). What makes a good image? Airbnb demand analytics leveraging interpretable image features. *Management Science*.
- Zhao, K., Hu, Y., Hong, Y., & Westland, J. C. (2019). Understanding Factors that Influence User Popularity in Live Streaming Platforms. Available at SSRN 3388949.
- Zhou, M., Chen, G. H., Ferreira, P., & Smith, M. D. (2021). Consumer Behavior in the Online Classroom: Using Video Analytics and Machine Learning to Understand the Consumption of Video Courseware. *Journal of Marketing Research*, 58(6), 1079-1100.

Online Appendix

Video Influencers: Unboxing the Mystique

Online Appendix A – Operationalization of Text Model

We provide an overview of the implementation of our Text Model - the BERT Framework (Devlin et al., 2018) in A.1, and explain the architecture of the encoders and attention mechanism (used in the BERT framework) in A.2 and A.3 respectively.

A.1 BERT Framework

The BERT model converts a sentence into word-piece tokens¹ as done by state-of-the-art machine translation models (Wu et al., 2016). Furthermore, the beginning of each sentence is appended by the ‘CLS’ (classification) token and the end of each sentence is appended by the ‘SEP’ (separation token). For example, the sentence ‘Good Morning! I am a YouTuber.’ will be converted into the (word-pieces or) tokens [‘[CLS]’, ‘good’, ‘morning’, ‘!’, ‘i’, ‘am’, ‘a’, ‘youtube’, ‘##r’, ‘.’, ‘[SEP]’]. A 768-dimensional initial embedding learnt for each token during the pre-training phase is passed as input to the model, and is represented by the vector x_m in Figure A1, where m is the number of tokens in the longest sentence. This vector x_m has pre-learned contextual embeddings that will aid the model in capturing relationships with our four outcome variables.

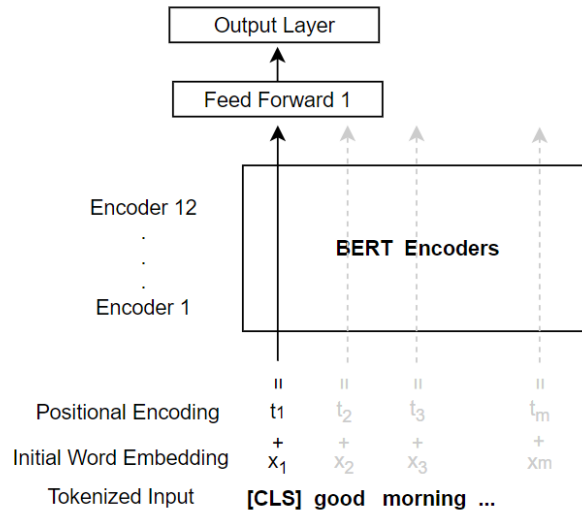


Figure A1: BERT Framework

The token embedding is combined with a positional encoder t_m that codes the position of the token in the sentence using sine and cosine functions (see Devlin et al. (2018) for details). This is passed through a set of 12 encoders arranged sequentially. The output of the ‘CLS’ token is passed through the

¹ We use the BERT-base-uncased model (that converts all words to lower case and removes accent markers) as compared to the cased model, because the uncased model is known to typically perform better unless the goal is to study case specific contexts such as ‘named entity recognition’ and ‘part-of-speech tagging.’

feed forward 1 layer that is initialized with pre-trained weights from the next sentence prediction task, and has a *tanh* activation function. We follow this up with an output layer that connects with either of our three continuous outcomes or binary outcome. We then fine-tune the entire model with all hierarchical layers over our data sample.

The Encoders (explained in A.2) contain the self-attention heads (explained in A.3) which help the model capture the relative importance between word-pieces while forming an association with the outcome of interest. By virtue of being pre-trained to capture contextual usage of words, the model is able to make better decisions on assigning relative attention (importance) weights to different word-pieces (tokens) in our sample. Word-pieces that receive more attention play a more important role (in either a positive or negative direction) in predicting the outcome of interest. We analyze these attention weights during ex-post interpretation.

A.2 BERT Encoders

BERT Encoders comprise a set of 12 sequentially arranged identical encoders, and we illustrate the architecture of one encoder in Figure A2.²

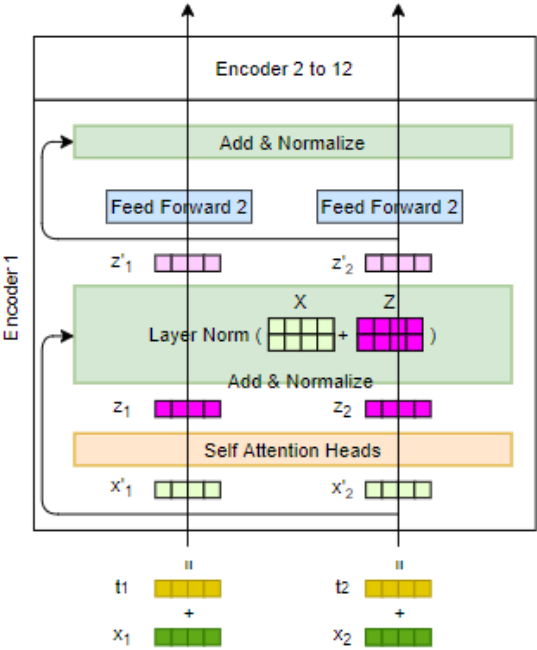


Figure A2: Encoders

We explain an example with a sentence that has only two tokens, and this can be extended to any example that has a maximum of 512 tokens, which is the maximum limit of the pre-trained BERT model.

² Our figures are inspired by the work of Jay Alammar (see Alammar (2018) for more details).

The combined vector of the initial token embedding (x_1, x_2) and positional encoding (t_1, t_2) results in the vectors (x'_1, x'_2) that are passed through self-attention heads which incorporate information of other relevant tokens into the focal tokens. The architecture of the self-attention head is explained in A.3. The outputs of the self-attention head (z_1, z_2) are then added with the original input (x'_1, x'_2) using a residual connection (shown with a curved arrow) and normalized (using mean and variance). The outputs (z'_1, z'_2) are passed through identical feed forward networks that have a GELU (Gaussian Error Linear Unit) activation function, i.e. $gelu(x) = 0.5x \left(1 + erf \left(\frac{x}{\sqrt{2}} \right) \right)$. The gelu activation combines the advantages of the ReLU (Rectified Linear Unit) non-linearity (i.e., $relu(x) = max(0, x)$) with dropout regularization. The outputs of the feed forward network are added with the inputs (z'_1, z'_2) using a residual connection and normalized again before being fed to the next encoder in sequence. In addition, each sub-layer is first followed by a dropout probability of 0.1 before being added and normalized.

A.3 BERT Attention Mechanism: Self-Attention heads

Next, we explain the self-attention heads that are illustrated in Figure A3. There are 12 self-attention heads that capture the contextual information of each token in relation to all other tokens used in the text. In other words, this allows the model to identify and weigh all other tokens in the text that are important when learning the vector representation of the focal token. We use this to measure the importance (strength) of association between the tokens in the text and the outcome of interest.

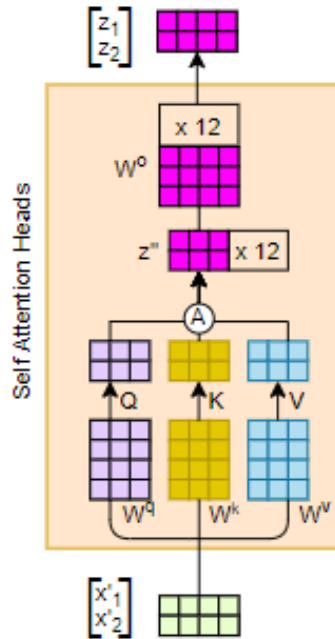


Figure A3: Self-Attention Heads

The inputs (x'_1, x'_2) are concatenated and multiplied with three weight matrices, W^q, W^k and W^v (that are fine-tuned during model training) to get three vectors – Q (Query), K (Key) and V (Value). These three vectors are combined using an attention function (A):

$$A(Q, K, V) = z''_0 = \text{softmax}\left(\frac{Q \cdot K^T}{\sqrt{d_k}}\right) \cdot V$$

where, d_k , the dimension of the Key vector, is 64 and is equal to the dimensions of the other two vectors d_q and d_v ; and $\text{softmax}(x) = \frac{e^{x_i}}{\sum_{i=1}^m e^{x_i}}$. The division by $\sqrt{d_k}$ is performed to ensure stable gradients. The computation of z''_0 is for one attention head, and this is carried out in parallel for 11 additional attention heads to give us 12 vectors, $z''_0 \dots z''_{12}$, which are concatenated to produce z'' . This is multiplied with a weight vector W^o (which is fine-tuned during model training) to produce output (z_1, z_2) . The use of 11 additional attention heads allows the model to capture more complex contextual information.

In order to capture the estimated attention weights, we average the output across all the attention heads in the last encoder of the BERT model, which results in an attention vector of dimension $\langle n, k, k \rangle$ where n is the number of videos used in the analysis, and $\langle k, k \rangle$ corresponds to k weights for k tokens, where k equals the maximum number of tokens (word-pieces) for a covariate type – title, description (first 160 characters) or captions/transcript (beginning, middle or end). As mentioned in A.1, the first token for each example is the ‘CLS’ or classification token. We are interested in the attention weights corresponding to this token because the output from this token goes to the output layer (as shown earlier in Figure A1). Thus, we get at an attention weight vector of dimension $\langle n, k \rangle$, where each observation has k weights corresponding to the ‘CLS’ token. We exclude ‘CLS’, ‘SEP’ and any token used for padding short sentences), during ex-post interpretation.

Online Appendix B – Operationalization of Audio Model

We provide an overview of the implementation of our Audio Model – YAMNet +Bi-LSTM+ Attention Mechanism in B.1, and explain the architecture of MobileNet v1 in B.2 and Bi-LSTM with attention mechanism in B.3.

B.1 YAMNet +Bi-LSTM+Attention Mechanism

We analyze audio data using the pre-trained YAMNet model (Pilakal & Ellis, 2020), and customize it with an additional Bidirectional LSTM (Bi-LSTM) layer and an attention mechanism as shown in the framework in Figure B1.

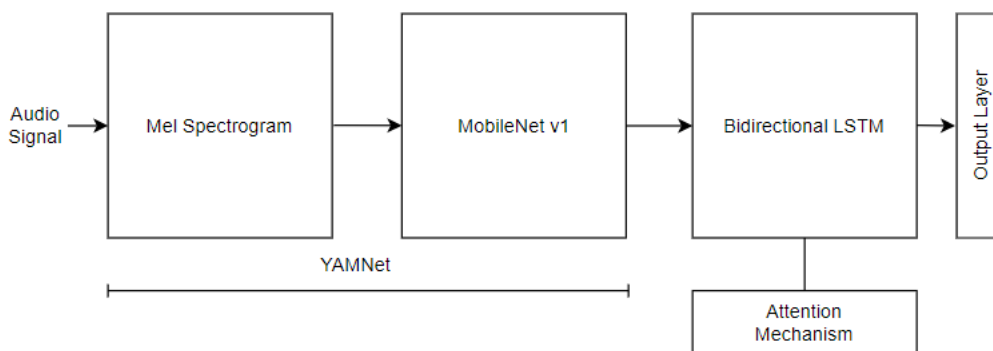


Figure B1: Audio Model Framework

Each audio signal is a 30 second clip, which we resample at 16,000 Hz and mono sound (for consistency), and this results in 480,000 data points for each clip. Note that for a few influencer videos that are shorter than 30 seconds, we append it with moments of silence to make the audio length consistent across our sample. To summarize the large number of data points, the model first generates a Mel spectrogram that spans the frequency range of 125 to 7500Hz (note that the 2000-5000 Hz range is most sensitive to human hearing (Widex, 2016)) over which the YAMNet model has been pre-trained. The spectrogram uses the pre-trained Short-Term Fourier Transform window length of 25ms with a hop size of 10ms that results in a 2998 x 64 (time steps x frequency) vector corresponding to 30 seconds of each audio clip. This corresponds to 64 equally spaced Mel bins on the log scale, such that sounds of equal distance on the scale also sound equally spaced to the human ear. The model then passes each segment of 960ms from the spectrogram output, i.e., 96 frames of 10ms each with overlapping patches (to avoid losing information at the edges of each patch) as input to the MobileNet v1 architecture. The size of the overlap or hop size is 490ms, which results in a total of 60 moments for each 30 second audio clip.

The MobileNet v1 (explained in B.1) processes the spectrogram through multiple mobile convolutions and returns audio class predictions for each of the 60 moments in the clip. This comprise a total of 521 different audio classes such as speech, music, animal, etc. (corresponding to each 960 ms

segment) over which the model has been pre-trained. Pilakal and Ellis (2020) remove 6 audio classes (viz. gendered versions of *speech* and *singing*; *battle cry*; and *funny music*) from the original set of 527 audio classes to avoid potentially offensive mislabeling.

We then pass the $\langle 521 \times 60 \rangle$ dimensional vector as input to the Bi-Directional LSTM layer with an attention mechanism. We make this layer bidirectional to allow it to capture the interdependence between sequential audio moments from both directions. For example, the interdependence between the sound of a musical instrument at 5 seconds and the beginning of human speech at 15 seconds can be captured by the model bidirectionally. We adapt the attention mechanism used for neural machine translation by Bahdanau et al. (2014) (explained in B.3) to help the Bi-LSTM model capture the relative importance between sound moments in order to form an association with an outcome. These measures of relative importance (attention) can be understood similarly as the attention weights in the Text model, and are analyzed during ex-post interpretation. We pass the output of the Bi-LSTM (with attention mechanism) through an output layer which connects with either of our three continuous outcomes or binary outcome. We then fine-tune the Bi-LSTM with attention mechanism over our data sample.

B.2 MobileNet v1 architecture

The MobileNet v1 architecture is illustrated in detail in Table B1 (Howard et al., 2017). Each row describes Stage i with input dimension $[\hat{H}_i, \hat{W}_i]$ (resolution), output channels \hat{C}_i and \hat{L}_i layers (depth).

Stage i	Operator \hat{F}_i	Input Resolution $(\hat{H}_i \times \hat{W}_i)$	Output Channels \hat{C}_i	Depth \hat{L}_i (Layers)	Pre-trained Weights
1	Conv, k3x3, s2	96 x 64	32	1	Yes
2	MConv, k3x3, s1	48 x 32	64	1	
3	MConv, k3x3, s2	48 x 32	64	1	
4	MConv, k3x3, s1	24 x 16	128	1	
5	MConv, k3x3, s2	24 x 16	128	1	
6	MConv, k3x3, s1	12 x 8	256	1	
7	MConv, k3x3, s2	12 x 8	256	1	
8	MConv, k3x3, s1	6 x 4	512	5	
9	MConv, k3x3, s2	6 x 4	512	1	
10	MConv, k3x3, s2	3 x 2	1024	1	
11	Global Average Pooling	3 x 2	1024	1	
12	Dense	1 x 1	521	1	

Table B1: MobileNet-v1 architecture

Stage 1 has a regular convolution operation, whereas Stage 2 to 10 have the Mobile Convolution which is the main building block of the architecture. It is represented as “MConv, $k \times k$, s ” where $k \times k = 3 \times 3$ is the size of the kernel and $s = \{1,2\}$ is the stride. MConv divides the regular convolution operation into

two steps – depth wise separable convolutions and point wise convolution, thus increasing the speed of computation (see Howard et al. (2017) for details). Stage 11 has a Global Average Pooling Layer that averages the inputs along its height and width and passes its output to Stage 12 which is a Dense output layer with 521 logistic functions that give the per class probability score corresponding to the 960 ms input segment. We use a hop size of 490 ms so that we get an even number of 60 time step predictions corresponding to the 30 seconds of input. The resulting output vector has a dimension of 521x60 (audio classes x time steps) for each 30 second clip.

B.3 Bi-LSTM with Attention

The output from MobileNet v1 is passed as input to the Bi-LSTM with attention mechanism, shown in Figure B2.

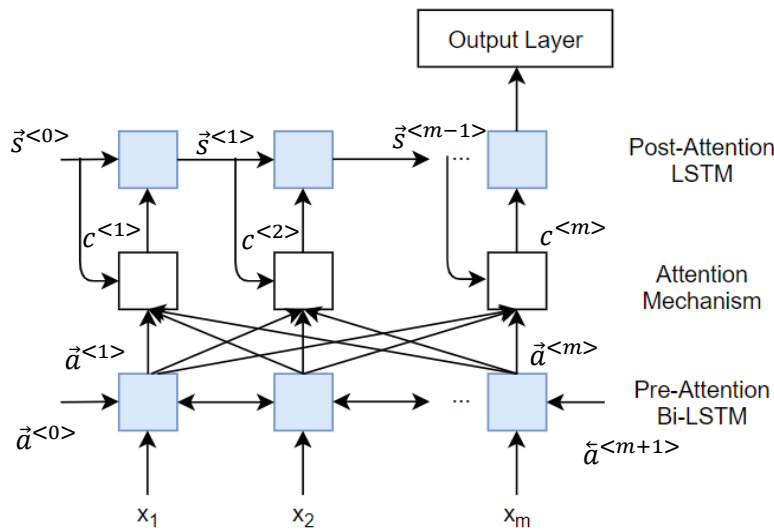


Figure B2: Bi-LSTM with Attention

We use two layers of LSTM cells – the first layer is a 32-unit Bidirectional LSTM layer and the second layer is a 64-unit (unidirectional) LSTM layer. They are separated by an attention mechanism as shown in the figure. Each audio segment $x_m \langle 521, 1 \rangle$, where m is the total number of moments (time steps), is passed as input to each cell of the Bidirectional LSTM layer. This layer is made bidirectional to allow it to capture the interdependence between sequential audio segments from both directions. The sequential nature of LSTM cells in a layer allow the model to capture dependencies between audio segments that are separated from each other (see the LSTM paper by Gers et al. (1999) for more details). We adopt the attention mechanism used for neural machine translation by Bahdanau et al. (2014) to help the Bi-LSTM model focus on more important parts of the input. The mechanism weighs the output activations ($a^{<t>} = [\vec{a}^{<t>}, \vec{a}^{<t>}]$, $t = 1$ to m) from each cell of the pre-attention Bi-LSTM layer before passing the contextual output, $c^{<t>}$, to the post-attention LSTM layer above it. In addition, each cell of

the attention mechanism takes as input the output activation $s(t - 1)$ from each preceding cell of the post-attention LSTM layer which allows it to factor in the cumulative information learnt by the model till that time step (see Bahdanau et al. (2014) for more details on the attention mechanism). The output of the last cell in the post-attention LSTM layer is passed to an output layer which has a linear activation function for the three continuous outcomes and a sigmoid activation function for the binary outcome. The context vector $c^{<m>}$ from the last cell of the attention mechanism allows measurement of the relative weights placed by the model along the time dimension of the input in order to form an association with the outcome of interest. Audio moments that have higher weight are more important while forming an association between the audio clip and the outcome.

Online Appendix C – Operationalization of Image Model

We provide an overview of the implementation of our Image Model – VGG-16 +Bi-LSTM in C.1. We then explain the architecture of VGG-16 in C.2, the architecture to combine information from all video frames in C.3, and our approach to find gradient-based salient areas in C.4.

C.1 VGG-16 + Bi-LSTM

We use VGG-16 to analyze thumbnail images and a combination of VGG-16 and Bi-LSTM to analyze video frames. First, we pass thumbnail images as input to one VGG-16, and then finetune its final layers to capture relationship with each outcome. We provide details on the VGG-16 architecture in C.2. Next, we illustrate in Figure C1 our framework to analyze video frames. We pass each image frame $i = 1$ to m , where m has a maximum value of 30 frames, through a VGG-16 architecture. Our sampling rate of one frame per second (30 frames in 30 seconds) in conjunction with the size of our data sample (1620 videos) ensures that our model is feasible to analyze.

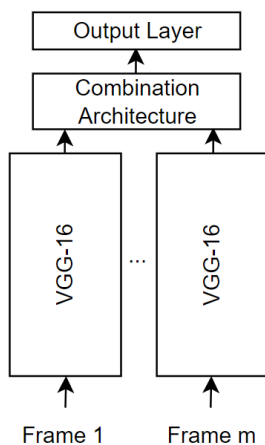


Figure C1: Framework to analyze Video Frames

In the last step, we combine the outputs from each VGG-16 model. Our combination architecture comprises the Bi-LSTM, known to be one of the best performing architectures at capturing sequential information from video frames (c.f. Yue-Hei Ng et al. (2015)). We compare its performance with another high performing architecture, Max Pooling followed by Global Average Pooling (Max-GAP), that preserves spatial information across video frames. The output of the combination architecture is passed through an output layer which connects with either of our three continuous outcomes or binary outcome. We explain the combination architecture and fine-tuning process in more detail in C.3.

C.2 VGG-16 Architecture

VGG-16 has 16 layers whose parameters can be learned (Simonyan & Zisserman, 2014). The architecture of VGG-16, customized to our input dimension of $135 \times 240 \times 3$ (where 3 corresponds to pixel intensities

for Red, Green and Blue channels), is shown in Table C1. Each row describes Stage i with input dimension $[\hat{H}_i, \hat{W}_i]$ (resolution), output channels \hat{C}_i and \hat{L}_i layers (depth).

Stage i	Operator \hat{F}_i	Input Resolution $(\hat{H}_i \times \hat{W}_i)$	Output Channels \hat{C}_i	Depth \hat{L}_i (Layers)	Pre-trained ImageNet weights
1	Conv, k3x3, s1	135 x 240	64	2	Yes
2	Max Pooling, k2x2, s2	135 x 240	64	1	
3	Conv, k3x3, s1	67 x 120	128	2	
4	Max Pooling, k2x2, s2	67 x 120	128	1	
5	Conv, k3x3, s1	33 x 60	256	3	
6	Max Pooling, k2x2, s2	33 x 60	256	1	
7	Conv, k3x3, s1	16 x 30	512	3	
8	Max Pooling, k2x2, s2	16 x 30	512	1	
9	Conv, k3x3, s1	8 x 15	512	3	
10	Max Pooling, k2x2, s2	8 x 15	512	1	
11	Global Average Pooling	4 x 7	512	1	No
12	Dense	1 x 1	1	1	

Table C1: VGG-16 architecture

Stages 1, 3, 5, 7 and 9 have convolution operations, whereas Stages 2, 4, 6, 8 and 10 have the max pooling operation, where $k \times k = 3 \times 3$ is the size of the kernel and $s = \{1,2\}$ is the stride. To analyze thumbnails, we use the pre-trained weights from Stage 1 to 10, and tune the weights of Stage 11 and 12. Stage 11 has a Global Average Pooling Layer that averages the inputs along its height and width and passes its output to Stage 12 which is a Dense output layer. The output layer has a linear activation function for the three continuous outcomes and a softmax activation function for the binary outcome.

C.3 Combination Architectures

To analyze video frames ($i = 1$ to m , where m has a maximum value of 30) we use the Bi-LSTM architecture that captures sequential information across different video frames. This is illustrated in Figure C2. Each VGG-16 architecture takes a unique video frame as input and provides the output from Stage 10 to the Global Average Pooling (GAP) Layer. This is followed by Dense Middle Layers (that use ReLU activation for continuous outcomes and sigmoid activation for the binary outcome), which is followed by a single Bi-LSTM layer with 256 memory cells, and finally a Dense output layer (that uses linear activation for continuous outcomes and softmax activation for the binary outcome). We compare its performance with the Max-GAP architecture that preserves the spatial information across different video frames. This is illustrated in Figure C3. It finds the maximum value across the Stage 10 output from each of the 30 VGG-16 architectures $[4 \times 7 \times 512 \times 30 \text{ frames}]$ and returns an array of shape $[4 \times 7 \times 512]$. This is followed by a GAP layer that reduces the dimensions to $[1 \times 1 \times 512]$. While using both

combination architectures, we use the pre-trained ImageNet weights (Krizhevsky et al., 2012) from Stage 1 to 10 in each VGG-16 architecture and then we finetune the weights of the top layers.

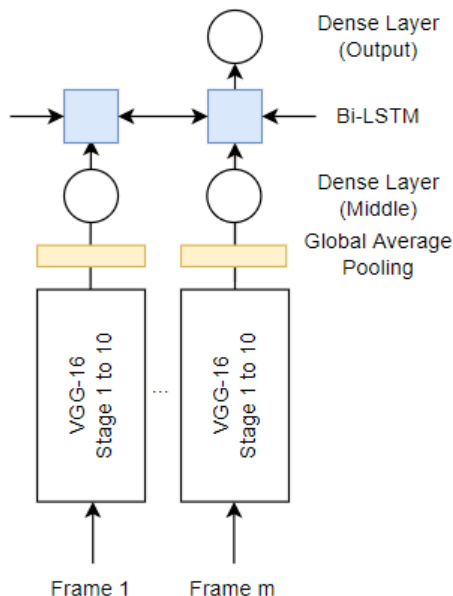


Figure C2: Bi-LSTM Combination

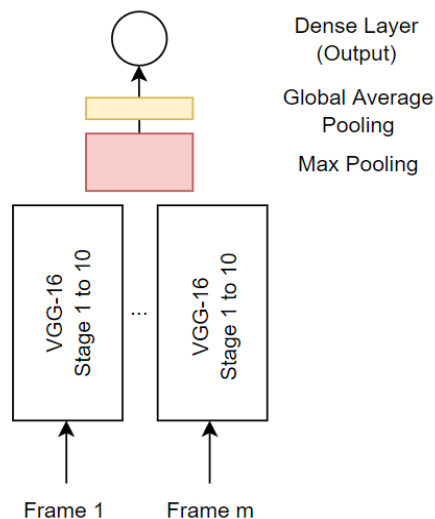


Figure C3: Max-GAP

C.4 Gradient-based saliency

As our VGG-16 model uses pretrained weights from the ImageNet classification task, the lower layers of the model are well trained to detect basic attributes of objects in images. This helps the model differentiate between various objects in the images of our video sample during the process of finetuning. After the end of model training, we ex-post identify the salient parts of images that are associated with an outcome through gradient-based activation maps (cf. Selvaraju et al., 2017). We find gradients by taking the derivative between the predicted continuous outcome (or class of predicted binary outcome) and the output of the activation layer after the last convolution layer in each VGG-16 architecture that processes one video frame. However, unlike Selvaraju et al. (2017), we do not apply the ReLU (Rectified Linear Unit) activation on the gradient values as we would like to retain negative gradient values for interpretation. Hence our approach is a modified gradient-based activation map that is suitable for our setting. Areas of the image with positive (negative) gradients correspond to regions that are positively (negatively) associated with continuous outcomes and the predicted class of loveability.

Online Appendix D – Comparison of Model Performance

We compare individual models with benchmarks in D.1 and compare different combined models in D.2.

D.1 Comparison of Individual Models with Benchmarks

We compare the predictive performance of our individual models for Text, Audio and Images with standard benchmarks used in the marketing literature to demonstrate that our models do not compromise on predictive ability³. To make this comparison, we choose the two outcome measures of deep engagement: commentability (continuous outcome) and loveability (binary outcome). For the unstructured covariates, we focus on the beginning 30 seconds of video data (Tables D1, D2 and D4) in addition to title, description (first 160 c) and thumbnails.

We first compare the predictive performance of the Text Model (BERT) with four standard models in Table D1. These standard benchmarks include an LSTM (with a 300 dimensional Glove word vector embedding), CNN model (Liu et al., 2019), CNN-LSTM (Chakraborty et al., 2022) and CNN-Bi-LSTM. As can be seen in Table D1, BERT performs better than the benchmarks while predicting both commentability (lowest RMSE) and loveability (highest accuracy).

Outcome	Covariate	LSTM	CNN	CNN-LSTM	CNN-Bi-LSTM	BERT
Commentability	Title	0.99	0.91	0.90	0.88	0.68
	Description (first 160c)	0.98	0.93	0.89	0.88	0.77
	Captions/transcript (beginning 30s)	0.97	1.04	0.94	0.93	0.85
Loveability	Title	0.67	0.70	0.70	0.70	0.72
	Description (first 160c)	0.50	0.69	0.69	0.69	0.70
	Captions/transcript (beginning 30s)	0.67	0.70	0.70	0.70	0.71

Table D1: Comparison of Text Model predictive performance on holdout sample for measures of deep engagement (RMSE for commentability; Accuracy for loveability)

We now compare the model performance of the Audio model with other variants that are devoid of transfer learning and attention, and present the results in Table D2. First, we find that the addition of the transfer learned MobileNet v1 to a model that uses only the Mel Spectrogram + Bi-LSTM results in improved RMSE when predicting commentability and improved accuracy when predicting loveability. Addition of the attention mechanism to this results in our Audio model which has improved RMSE when predicting commentability but does not have improved accuracy when predicting loveability. Overall, our Audio model performs the best in out-of-sample prediction, thus demonstrating that transfer learning (via MobileNet v1) and capturing relative attention weights (via the attention mechanism) also contribute towards the predictive ability of the model (in addition to helping with interpretation).

³ We run all the standard benchmark models at least three times and average their prediction errors. We run our main models for Text and Audio (and Image) 50 (and 25) times and average their prediction errors.

Outcome	Covariate	Mel Spectrogram + Bi-LSTM	Mel Spectrogram + MobileNet v1 + Bi-LSTM	Audio Model: Mel Spectrogram + MobileNet v1 + Bi-LSTM + Attention
Commentability	Audio (first 30s)	0.95	0.91	0.86
Loveability	Audio (first 30s)	0.59	0.64	0.64

Table D2: Comparison of Audio Model performance on holdout sample (RMSE for commentability; Accuracy for loveability)

Next, in Table D3, we compare the performance of the Image Model (VGG-16) with a simple 4-layer CNN model using thumbnail data. We see a substantial improvement in both RMSE and accuracy when using VGG-16, thus demonstrating the benefits of both transfer learning and a deeper architecture.

Outcome	Covariate	4-layer CNN	VGG-16
Commentability	Thumbnail	2.53	0.93
Loveability	Thumbnail	0.55	0.68

Table D3: Comparison of Image Model performance on holdout sample (RMSE for commentability; Accuracy for loveability)

Next, in Table D4, we compare the performance of our Image Model that uses the Bi-LSTM architecture to capture sequential information in video frames with an Image Model that uses the Max-GAP architecture (Online Appendix C.3) to capture spatial information in video frames. We find that the Bi-directional LSTM architecture which captures sequential information performs better than the Max-GAP architecture that captures only spatial information while predicting commentability (lower RMSE). However, both architectures perform equally well while predicting loveability. This demonstrates that capturing sequential information is more important for predicting commentability but not more important for predicting loveability. Overall, the Bi-LSTM architecture is better than the Max-GAP architecture, as it can predict both outcomes well.

Outcome	Covariate	Max-GAP	Bi-LSTM
Commentability	Video Frames (beginning 30s @ 1fps)	0.89	0.84
Loveability	Video Frames (beginning 30s @ 1fps)	0.66	0.66

Table D4: Comparison of Image Model performance with different combination architectures on holdout sample (RMSE for commentability; Accuracy for loveability)

D.2 Comparison of Different Combined Models

In Table D5, we compare the performance of different Combined Models (discussed earlier in Section 5.2) on the holdout sample. We use structured features and the average of the predicted values (across all bootstrap iterations) from each unstructured model as input to the Combined Model shown earlier in Eq (1). For the Combined Models, we test four linear models – OLS, Ridge Regression (L2 penalization), LASSO (L1 penalization), Elastic Net (0.5L1 and 0.5L2 penalization), and three non-linear models – Deep Neural Net (with three hidden layers), Random Forests and Extreme Gradient Boosting (XGBoost). We find that on average Ridge Regression has the best performance on the holdout sample for all the continuous outcomes (lowest RMSE) and the binary outcome - loveability (highest accuracy).

	Commentability	Loveability	Thumbsability	Likeability
OLS	0.78	0.74	0.63	0.77
Ridge Regression	0.73	0.74	0.56	0.71
LASSO	1.17	0.73	0.96	1.29
Elastic Net	1.12	0.74	0.91	1.20
Deep Neural Net	0.77	0.74	0.56	0.73
Random Forests	0.73	0.74	0.59	0.76
XGBoost	0.77	0.72	0.63	0.76

Table D5: Performance of different Combined Models on holdout sample (RMSE for commentability, thumbsability and likeability; Accuracy for loveability)

Online Appendix E – Details of Interpreting Text Model Results

We discuss our modeling choice of Ridge Regression to interpret the results of the Text Model in E.1, and then explain the interpretation results graphically in E.2.

E.1 Modelling Choice of Ridge Regression

Using Ridge Regression to interpret the relationships captured in the Text Model allows us to capture heterogeneity in effects across brands and emotional words. Additional reasons for our choice of Ridge Regression are as follows: (a) Some brands or emotional words may only be used once in our data and hence OLS cannot be used, (b) number of predictors $n_p > n$ for Eq (5) while interpreting the Text model, which makes Ridge Regression suitable, and (c) a limitation of other penalized regression methods such as LASSO is that it will cap variable selection at n variables (and not n_p) and hence we may miss out on capturing important predictors, (d) LASSO or Elastic Net may miss out on selecting some brands or emotional words if their effect is collinear with other brands or emotional words, (e) Ridge Regression shrinks the non-important predictors towards 0, thus allowing us to identify the relatively more important predictors.

We are able to estimate Eq (5) using OLS while modeling the predicted outcomes from the Audio or Image models because in these instances we do not model the heterogeneity across brands or emotional words. Instead, we use covariates for ‘number of brand mentions’ and ‘number of emotional word mentions’ because textual stimuli in this case are not features of interest and are only used as controls.

More concretely, we replace $\sum_{k=1}^{n_b} \beta_{1pk}(BITX_{it}) + \sum_{k=1}^{n_e} \beta_{2pk}(EITX_{it})$ in Eq (5) with $\beta_{1p}(\text{Number of brand mentions}_{it}) + \beta_{2p}(\text{Number of emotion mentions}_{it})$.

E.2 Graphical Illustration and Robustness of Interpretation Results of Text Model

We begin by showing a graphical illustration of Table 7 in Figure E1. The X axis shows the median value of brand/emotion coefficients (across 50 bootstrap iterations) from Step 1 of the analysis that correspond to a change in the attention weights. The Y axis shows the median value of brand/emotion coefficients (across 50 bootstrap iterations) from Step 2 of the analysis that correspond to a change in the predicted outcome. Our quadrants of interest are Quadrant 1 and 4 that have a positive X axis corresponding to an increase in attention directed to the brand/emotion. The brands/emotions in Quadrant 1 have a positive Y axis corresponding to an increase in the predicted outcome variable, whereas those in Quadrant 4 have a negative Y axis corresponding to a decrease in the predicted outcome variable. We label the data points for the brands/emotions in these quadrants whose coefficient value is at least 30% (threshold value) of the magnitude of the maximum coefficient value on each axis to avoid cluttering the figures with labels (Note that the results in Table 7 used a threshold of 5%). The values in brackets below the name of a

We now discuss how the results in Figure E1 (or Table 7) for the beginning 30s are robust to brands/emotions that have a small or a large effect on the engagement measures. We show this graphically in Figure E2. As can be seen, the green and brown lines do not intersect which demonstrates that the difference between the percentage of brands in Q1 and Q4 is in the same direction as we move along the respective X and Y axis of Figure E2. In other words, we demonstrate how our findings for the beginning 30s are robust to brands/emotions that have a small or a large effect on the engagement measures.

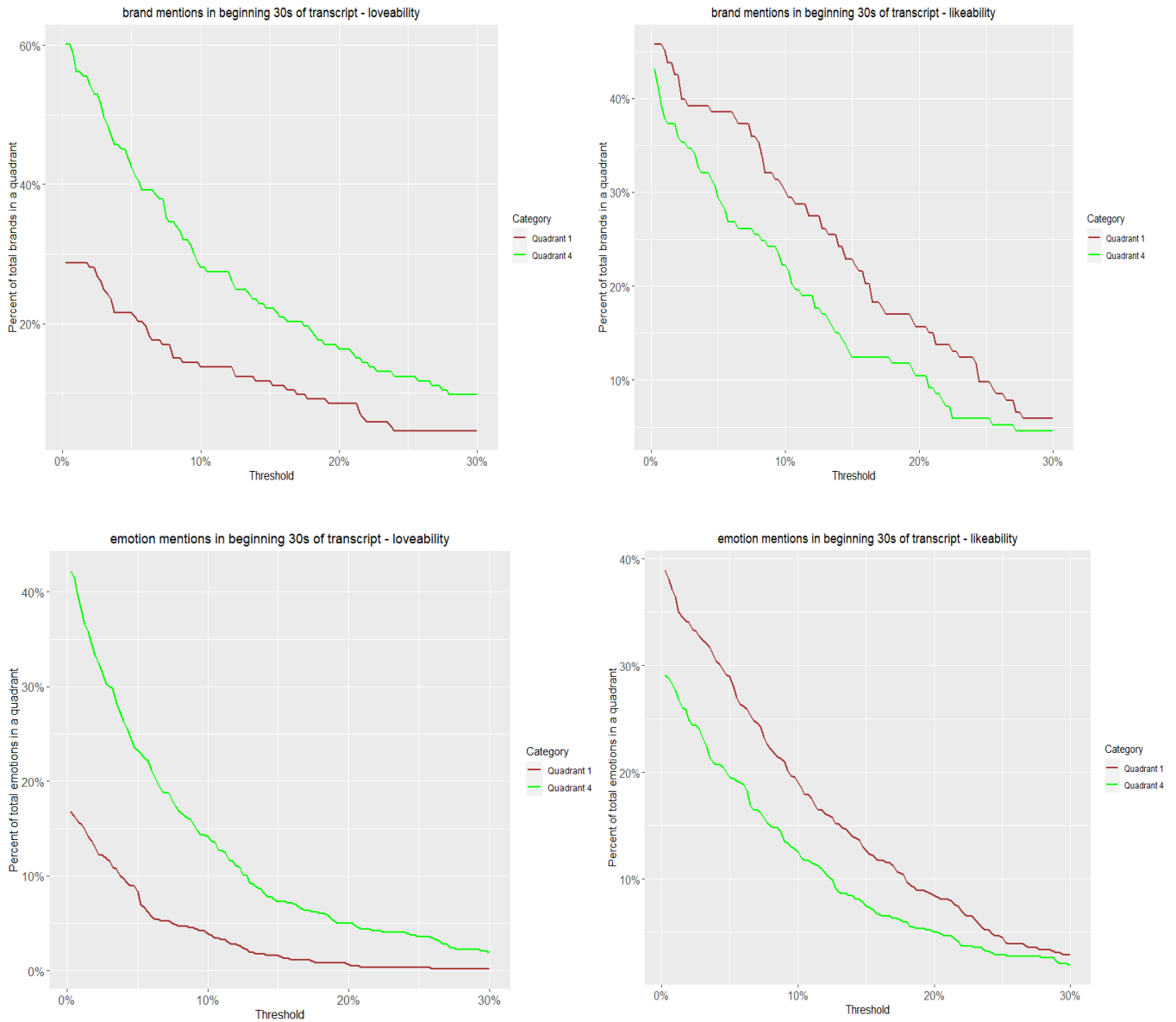


Figure E2: Robustness of interpretation results of Text Model for brand and emotion mentions in beginning 30 seconds

Online Appendix F – Simulations to Recover the True Data Generating Process

We conduct simulations to test whether our novel ex-post interpretation approach can recover the true data generating process. Specifically, we simulate an outcome (an engagement measure) to vary based on specific features in either text, audio or images. We then carry out model training as done in Section 7.1 using the covariates from our observed sample of data and the simulated outcome. We then follow this up with ex-post interpretation as done in Section 7.2. We implement bootstrap iterations 50 (25) times for the Text and Audio models (Image model) as done in Section 7. We explain in detail our simulation process for Text Model in F.1, Audio Model in F.2 and Image Model in F.3.

F.1 Simulations – Text Model

We first pick a covariate-outcome pair of interest, say “brand mentions in beginning 30 seconds of captions/transcript – likeability”. For those observations (of video t and influencer i) where a brand is *not* mentioned in the beginning 30 seconds, we generate a random normal distribution of log-likeability whose mean and standard deviation match the observed mean and standard deviation of our entire sample:

$$brand_absent_{it} \sim N(3.79, 1.11) \quad (F1)$$

For those observations (of video t and influencer i) where a brand is mentioned in the beginning 30 seconds, we generate a random normal distribution of log-likeability whose mean is twice the mean in Eq (F1) and standard deviation is half the standard deviation in Eq (F1):

$$brand_present_{it} \sim N\left(2 * 3.79, \frac{1.11}{2}\right) \quad (F2)$$

We can summarize our simulated outcome of log likeability, $Y_{simulated_{it}}$, for video t by influencer i , as follows:

$$Y_{simulated_{it}} = \begin{cases} N(3.79, 1.11) & \text{when brand is absent} \\ N\left(2 * 3.79, \frac{1.11}{2}\right) & \text{when brand is present} \end{cases} \quad (F3)$$

Our goal is to test whether our Text model assigns more attention to brand names (Step 1) while associating them with an increase in predicted likeability (Step 2). This should be expected to occur as the second distribution (Eq F2) has twice the mean and half the standard deviation as the first distribution (Eq F1). As done in Section 7.1, we first train our models on the training sample using the simulated outcome and our observed covariates. Next, as done in Section 7.2, we estimate equations (2) and (5) over the entire sample for each bootstrap iteration (50 times). We show the results in Figure F1. As can be seen in

the figure, brands are more often present in Quadrant 1 (increase in attention and an increase in predicted likeability). We also summarize the information from the figure in Table F1. As can be seen in the table, brands that meet the 5% threshold (same threshold used earlier in Table 7) more often lie in Quadrant 1. Furthermore, the average frequency with which all brands (in the beginning 30 seconds that meet the 5% threshold) remain in quadrant 1 across 50 bootstrap iterations is very high (91% X+, 97% Y+). The high percentage value demonstrates that we are able to mitigate concerns of model brittleness because of random model convergence to a local optimum during an iteration of model training. By bootstrapping over 50 iterations, we observe that the brand coefficients converge towards a dominant directional effect (Quadrant 1).

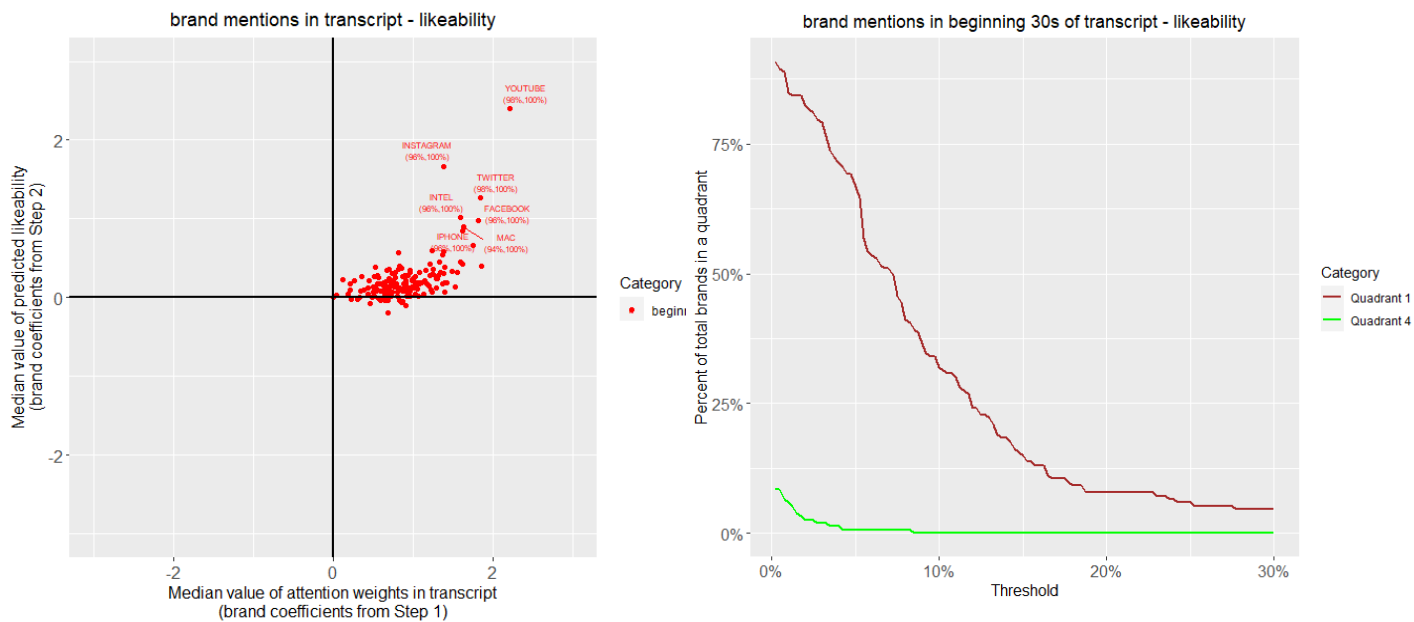


Figure F1: Interpretation results of simulation – Text Model

Figure F2: Robustness of Interpretation Results of Simulation – Text Model

Part of video	Quadrant	(Eq 1) Attention Weights (Step 1)	(Eq 5) Predicted Outcome (Step 2)	Likeability
Beginning	Q1	+	+	66.7%
	Q4	+	-	0.7%
	Q2	-	+	0.0%
	Q3	-	-	0.0%
Threshold: 5%				

Table F1: Interpretation Results of Simulation – Text model

These results are robust as the difference between the percentage of brands in Q1 and Q4 continue to hold true across a range of values of the threshold. We show this in Figure F2. As can be seen, the green and brown lines do not intersect which demonstrates that the difference between the percentage of brands in Q1 and Q4 is in the same direction as we move along the respective X and Y axis of Figure

F1. Hence, our findings are robust to brands that have a small or a large effect on likeability. Thus, we have shown that our ex-post interpretation approach using text data is able to recover the true data generating process.

F.2 Simulations – Audio Model

As done above, we first pick a covariate-outcome pair of interest, say “music duration in beginning 30 seconds – commentability”. We then generate a random normal distribution of log-commentability (for video t by influencer i) whose minimum and maximum value match the observed minimum and maximum values in our entire sample:

$$v_{it} \sim \text{Uniform}(-11.42, -2.18) \quad (\text{F4})$$

We then generate the simulated outcome of log commentability, $Y_{\text{simulated}_{it}}$, for video t by influencer i as follows:

$$Y_{\text{simulated}_{it}} = v_{it} - 0.5 * \text{Sum of } CI(\text{Music})_{it} \quad (\text{F5})$$

where, $\text{Sum of } CI(\text{Music})_{it}$ is the duration of music sounds in the beginning 30 seconds in video t by influencer i .

Our goal is to test whether our Audio model assigns more attention to moments of music (Step 1) while associating that with a decrease in predicted commentability (Step 2). Specifically, we would like to recover the coefficient of -0.5 associated with a decrease in commentability during ex-post interpretation. As done in Section 7.1, we first train our models on the training sample using the simulated outcome and our observed covariates. Next, as done in Section 7.2, we estimate equations (3) and (5) over the entire sample for each bootstrap iteration (50 times). The median value (across 50 iterations) of the estimated coefficient for $\text{Sum of } CI(\text{Music})_{it}$ is -0.47^4 which is approximately equal to -0.5 . The estimated coefficient values for $\text{Sum of } CI(\text{Music})_{it}$ are significant 100% of the time across all 50 iterations (Step 2). This is supported by a significant increase in attention to moments of music at least 90% of the time across all iterations (Step 1). Thus, we are able to demonstrate that our ex-post interpretation approach using audio data is able to approximately recover the true data generating process.

F.3 Simulations – Image Model

As done above, we first pick a covariate-outcome pair of interest, say “size of human images in beginning 30 seconds – likeability”. We then generate a random normal distribution of log-likeability (for video t by

⁴ Note that this corresponds to a 37% decrease in commentability ($\exp(-0.47)-1$) when sound duration increases by one moment.

influencer i) whose minimum and maximum value match the observed minimum and maximum values in our entire sample:

$$w_{it} \sim Uniform(-0.92, 6.83) \quad (F6)$$

We then generate the simulated outcome of log likeability, $Y_{simulated_{it}}$, for video t by influencer i as follows:

$$Y_{simulated_{it}} = w_{it} + 0.25 * SizeObject(Human)_{it} \quad (F7)$$

where, $SizeObject(Human)_{it}$ is the mean across 30 frames of the percentage of the image occupied by all objects that are human images in video t made by influencer i .

Our goal is to test whether our Image model associates human pixels with an increase in mean gradient values (Step 1) and an increase in predicted likeability (Step 2). Specifically, we would like to recover the coefficient of +0.25 associated with an increase in likeability during ex-post interpretation. As done in Section 7.1, we first train our models on the training sample using the simulated outcome and our observed covariates. Next, as done in Section 7.2, we estimate equations (4) and (5) over the entire sample for each bootstrap iteration (25 times). The median value (across 25 iterations) of the estimated coefficient for $SizeObject(Human)_{it}$ is 0.13⁵ which is close to the true value of 0.25. The estimated coefficient values for $SizeObject(Human)_{it}$ are significant 100% of the time across all 25 iterations (Step 2). This is supported by a significant increase in mean gradient values of human images 100% of the time across all iterations (Step 1). Thus, we are able to demonstrate that our ex-post interpretation approach using image data is able to recover a closeness to the true data generating process.

⁵ Note that this corresponds to a 14% increase in likeability ($\exp(0.13) - 1$) when size of human images increases by one percent.

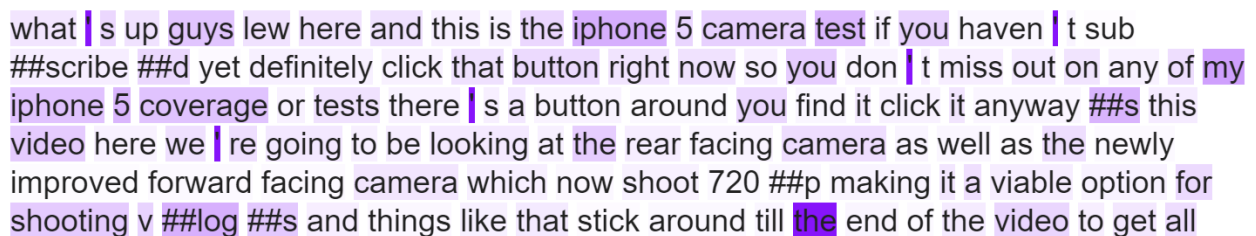
Online Appendix G – Details on Managerial Implications

In G.1, we discuss how to visualize the importance measures (attention weights for text and audio; and gradients for images) to help influencers identify areas for improvement. In G.2, we explain our process to decompose the variance explained by brand mentions while predicting likeability and loveability, so that marketers and brands can understand the overall impact of branded content in influencer videos.

G.1 Visual Illustration of Salient Regions in Text, Audio and Images

We discuss the process to visualize salient regions in unstructured data based on the results of our models in Section 5.1. These techniques can help influencers identify potential areas for improvement.

We illustrate an example of how text data can be visually interpreted. In Figure G1, we show the attentions weights on the captions/transcript (first 30s) from a video of a technology & business influencer. The words are tokenized into word-pieces in the figure as done by the model, and a darker background color indicates relatively higher attention weights. As can be seen in the figure, on average more attention is paid to the word ‘iphone’ than other words in the text. Note that the model assigns different attention weights to the word ‘the’ based on the context in which it is used (lower attention in the first line, but higher attention in the last line). While the model also assigns more attention to punctuation marks, such as the apostrophe, these associations may be spurious (as discussed earlier in Section 6) or may be confounded by word usage unique to the influencer which we control for during ex-post interpretation using influencer fixed effects (α_i) in equation (2). Our model predicts ‘not positive’ loveability for this clip (consistent with the findings in Table 7) and this matches the observed value.



what | s up guys lew here and this is the iphone 5 camera test if you haven | t sub
##scribe ##d yet definitely click that button right now so you don | t miss out on any of my
iphone 5 coverage or tests there | s a button around you find it click it anyway ##s this
video here we | re going to be looking at the rear facing camera as well as the newly
improved forward facing camera which now shoot 720 ##p making it a viable option for
shooting v ##log ##s and things like that stick around till the end of the video to get all

Figure G1: Attention weights in captions/transcript (first 30s) of a video

Next, we illustrate an example of how attention paid to audio moments in a video can be visually interpreted. We focus on the relationship between music and loveability. In Figure G2, we show the first 30 seconds of the audio clip of a travel influencer using four sub plots. The first plot shows the variations in the amplitude of the 30 second audio wave (sampled at 16 KHz) followed by the spectrogram of the wave where brighter regions correspond to stronger (or louder) amplitudes. Next, we show the interim output of the Audio model with the top 10 sound classes at each moment in the audio, where the darker squares indicate higher probability of observing a sound of that class at that moment. The last plot

displays the attention weights corresponding to each moment in the audio clip, where the darker squares indicate higher relative attention placed on that moment while forming an association with loveability. As can be seen in the figure, relatively more attention is directed to moments where there is music but no simultaneous speech. The model predicts positive loveability for this clip (consistent with the findings in Table 8) and this matches the observed value.

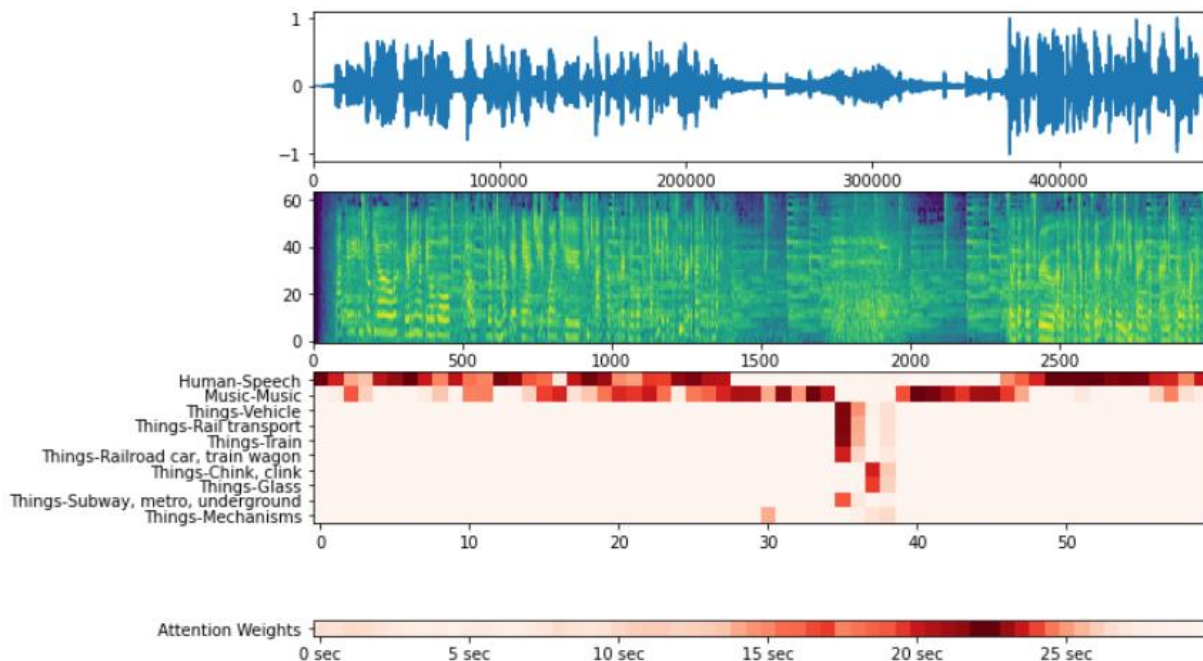


Figure G2: Attention weights in an audio clip (first 30 sec) of a video

Next, we illustrate how attention paid to image pixels on the video frames of a video can be visually interpreted. We show the first 15 frames @1fps for a video of a parenting influencer in Figure G3. The bottom of the figure shows the heat map (gradient values), where brighter (redder) regions are positively associated with likeability. We find that pixels associated with images of persons have brighter heat maps, and more attention is often paid to the whole image of the person than just the face of the person (e.g., Frame 3, 5, 6 and 7). This is correlated with the area below the face of the person where the influencer is gesturing with their hands. We can also note the attention paid to images of packaged goods in Frame 14 and 15. Also note that the model assigns high attention to all the pixels in Frames 1, 9 and 13, and hence they appear completely red. The predicted likeability for this example is 40 likes per dislike which is less than the median likeability of 54 likes per dislike. This can be expected given that the person is present in only around half the frames and the large size of packaged goods in the frames (which is consistent with the conclusions from Table 9).

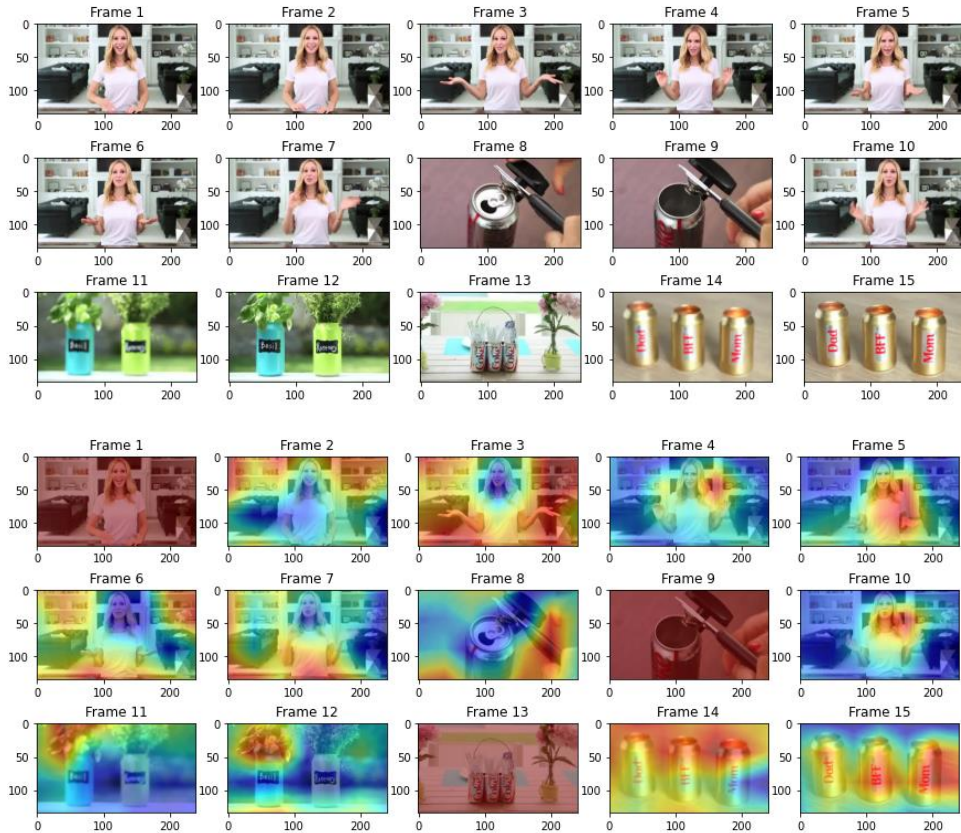


Figure G3: Gradient heat map in video frames (first 15 seconds) of a video

These visual illustrations for text, audio and images can help influencers and brand partners understand the potential influence of individual words, sound elements and objects in images. It can help them experiment with usage of different words, sounds and objects that can improve engagement with the video.

G.2 Decomposing Variance Explained by Brand Mentions

We decompose the variance explained by brand mentions in the relationship between captions/transcript in the beginning 30 seconds and likeability/loveability, and show the results in Table G1. We use the Ridge Regression model (used to interpret the Text Model in 7.2.1) to measure the ability of individual brands to predict the engagement measures. As shown in the table, we calculate the improvement in prediction performance over a standard baseline. For the baseline, we use the square root of the average of the total sum of squares for continuous outcomes or a prediction accuracy of 50% (random chance) for binary outcomes. We find that brand mentions in the beginning 30s explain 8.1% of the variance in likeability and perform 10% better than chance in predicting loveability. This demonstrates that brand mentions have a small but substantial role to play in explaining the behavior of both the sentiment of shallow and deep engagement. In the table, we also show the comparative performance of the Text model (BERT) (from Table 5). We find that the captions/transcript (beginning 30 sec) explain more of the

variance in likeability as well as loveability, but the improvement is much larger for loveability (310% as compared to 66%). This demonstrates that words other than brand names in captions/transcript (beginning 30 sec) explain a lot more variation in loveability than likeability.

Model	Outcome	Covariate	Holdout prediction error: $\sqrt{\frac{SSE}{n}}$ or accuracy	Holdout baseline: $\sqrt{\frac{SST}{n}}$ or chance accuracy	Percentage improvement over baseline (variance explained)	Relative performance improvement
Ridge Reg	Likeability	Individual indicators for each brand's mention in beginning 30s	1.02	1.11	8.1%	66%
BERT	Likeability	Captions/Transcript in beginning 30s	0.96	1.11	13.5%	
Ridge Reg	Loveability	Individual indicators for each brand's mention in beginning 30s	56%	50%	10%	310%
BERT	Loveability	Captions/Transcript in beginning 30s	71%	50%	41%	

Table G1: Variance explained by brand mentions

References to Online Appendix

- Alammar, J. (2018, June 27). *The Illustrated Transformer*. <http://jalammar.github.io/illustrated-transformer/>
- Bahdanau, D., Cho, K., & Bengio, Y. (2014). Neural machine translation by jointly learning to align and translate. *arXiv preprint arXiv:1409.0473*.
- Chakraborty, I., Kim, M., & Sudhir, K. (2022). Attribute sentiment scoring with online text reviews: Accounting for language structure and missing attributes. *Journal of Marketing Research*, 59(3), 600-622.
- Devlin, J., Chang, M.-W., Lee, K., & Toutanova, K. (2018). Bert: Pre-training of deep bidirectional transformers for language understanding. *arXiv preprint arXiv:1810.04805*.
- Gers, F. A., Schmidhuber, J., & Cummins, F. (1999). Learning to forget: Continual prediction with LSTM.
- Howard, A. G., Zhu, M., Chen, B., Kalenichenko, D., Wang, W., Weyand, T., Andreetto, M., & Adam, H. (2017). Mobilenets: Efficient convolutional neural networks for mobile vision applications. *arXiv preprint arXiv:1704.04861*.
- Krizhevsky, A., Sutskever, I., & Hinton, G. E. (2012). Imagenet classification with deep convolutional neural networks. *Advances in neural information processing systems*, 25.
- Liu, X., Lee, D., & Srinivasan, K. (2019). Large-scale cross-category analysis of consumer review content on sales conversion leveraging deep learning. *Journal of Marketing Research*, 56(6), 918-943.
- Pilakal, M., & Ellis, D. (2020). *YAMNet*. <https://github.com/tensorflow/models/tree/master/research/audioset/yamnet>
- Selvaraju, R. R., Cogswell, M., Das, A., Vedantam, R., Parikh, D., & Batra, D. (2017). Grad-cam: Visual explanations from deep networks via gradient-based localization. *Proceedings of the IEEE international conference on computer vision*,
- Simonyan, K., & Zisserman, A. (2014). Very deep convolutional networks for large-scale image recognition. *arXiv preprint arXiv:1409.1556*.
- Widex. (2016, August 9). *The human hearing range - what can you hear?* <https://www.widex.com/en-us/blog/human-hearing-range-what-can-you-hear>
- Wu, Y., Schuster, M., Chen, Z., Le, Q. V., Norouzi, M., Macherey, W., Krikun, M., Cao, Y., Gao, Q., & Macherey, K. (2016). Google's neural machine translation system: Bridging the gap between human and machine translation. *arXiv preprint arXiv:1609.08144*.
- Yue-Hei Ng, J., Hausknecht, M., Vijayanarasimhan, S., Vinyals, O., Monga, R., & Toderici, G. (2015). Beyond short snippets: Deep networks for video classification. *Proceedings of the IEEE conference on computer vision and pattern recognition*, 4694-4702.